Determination of the Structure Function F_2 at hermes

Dominik D. Gabbert
DESY-Zeuthen / Universität Hamburg

29. Oktober 2008

Probing the Structure of Nucleons

- **Deep-inelastic scattering** (DIS) plays major role in understanding of nucleon structure
- Lepton-nucleon scattering **cleanest way** to probe substructure of nucleon
- Exchange of virtual boson, **breakup** and hadronization in DIS regime

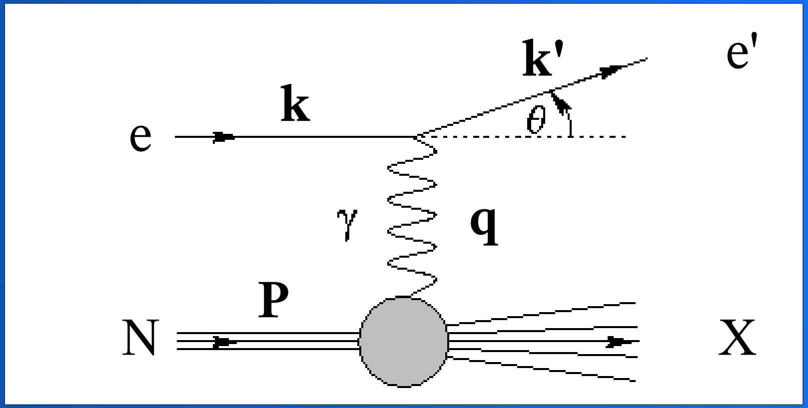

center-of-mass energy (e N)

$$s=(P+k)^2=M^2+2\mathrm{ME}$$

For given s, two kinematic variables completely describe the scattering process in the inclusive analysis, e.g.:

$$Q^2=-q^2=(k-k')^2=4\mathrm{EE}'\sin^2\frac{\theta}{2}$$ photon virtuality

$$\nu=\frac{P\cdot q}{M}=E-E'$$ photon energy (lab)

or

$$x=\frac{Q^2}{2\,P\cdot q}=\frac{Q^2}{2\,M\,\nu}$$ Bjørken scaling variable

$$y=\frac{P\cdot q}{P\cdot k}=\frac{\nu}{E}$$ inelasticity

Invariant mass of hadronic final state:

$$W^2=(P+q)^2=M^2+2\mathrm{M}\nu-Q^2$$

Resolution of deep-inelastic scattering:

$$\lambda=\frac{1}{|\boldsymbol{q}|}=\frac{1}{\sqrt{\nu^2+Q^2}}\approx\frac{2\mathrm{Mx}}{Q^2}$$

Structure Functions of the Nucleon

Deep-inelastic scattering in the *one-photon* exchange approximation can be written as:

$$\frac{d^2\sigma}{d\Omega\, dE'} = \frac{\alpha_{em}^2}{2MQ^2}\,\frac{E'}{E}\, L_{\mu\nu} W^{\mu\nu}$$

Leptonic and hadronic tensors have symmetric (S) and anti-symmetric (A) contributions:

$$\frac{d^2\sigma}{d\Omega\, dE'} = \frac{\alpha_{em}^2}{2MQ^2}\,\frac{E'}{E}\left[L_{\mu\nu}^{(S)} W^{\mu\nu(S)} + L'^{(S)}_{\mu\nu} W^{\mu\nu(S)} + L_{\mu\nu}^{(A)} W^{\mu\nu(A)} + L'^{(A)}_{\mu\nu} W^{\mu\nu(A)}\right]$$

Leptonic tensor known from QED.
Hadronic tensor describes a-priori unknown hadronic structure, parameterized by:

$W_{\mu\nu}^{(A)}$	Observable in polarized scattering	G_1, G_2 (or g_1, g_2)
$W_{\mu\nu}^{(S)}$	Observable in unpolarized scattering	W_1, W_2 (or F_1, F_2)

Structure Functions of the Nucleon

Deep-inelastic scattering in the *one-photon* exchange approximation can be written as:

$$\frac{d^2\sigma}{d\Omega\, dE'} = \frac{\alpha_{em}^2}{2MQ^2}\,\frac{E'}{E}\, L_{\mu\nu} W^{\mu\nu}$$

Leptonic and hadronic tensors have symmetric (S) and anti-symmetric (A) contributions:

$$\frac{d^2\sigma}{d\Omega\, dE'} = \frac{\alpha_{em}^2}{2MQ^2}\,\frac{E'}{E}\,[L_{\mu\nu}^{(S)} W^{\mu\nu(S)} + L'^{(S)}_{\mu\nu} W^{\mu\nu(S)} + L_{\mu\nu}^{(A)} W^{\mu\nu(A)} + L'^{(A)}_{\mu\nu} W^{\mu\nu(A)}]$$

Leptonic tensor known from QED.
Hadronic tensor describes a-priori unknown hadronic structure, parameterized by:

$W_{\mu\nu}^{(A)}$	Observable in polarized scattering	G_1, G_2 (or g_1, g_2)
$W_{\mu\nu}^{(S)}$	Observable in unpolarized scattering	W_1, W_2 (or F_1, F_2)

Consider unpolarized scattering in the following.
Parameterize hadronic structure using F_1 and F_2 for which Bjørken predicted scaling:

$$F_1(x,Q^2) = MW_1(\nu,Q^2) \rightarrow F_1(x) \qquad F_2(x,Q^2) = \nu W_2(\nu,Q^2) \rightarrow F_2(x)$$

$$\frac{d^2\sigma}{dx\, dQ^2} = \frac{4\pi\alpha_{em}^2}{Q^4}\left[y^2 \boldsymbol{F_1}(x,Q^2) + \left(1 - y - \frac{My}{2E}\right)\cdot \boldsymbol{F_2}(x,Q^2)\right]$$

Structure Functions F_1, F_2

In naïve Quark-Parton-Model:

$$F_1 = \frac{1}{2}\sum_f e_f^2[q(x)+\bar{q}(x)]$$
$$F_2 = x\sum_f e_f^2[q(x)+\bar{q}(x)]$$

Callan-Gross relation

$$F_2 = 2x\,F_1$$

Longitudinal (σ_L) and transverse (σ_T) virtual-photon contributions:

$$F_1 = \frac{MK}{4\pi\alpha_{em}}\sigma_T \qquad F_2 = \frac{\nu K(\sigma_L+\sigma_T)}{4\pi\alpha_{em}(1+Q^2/4M^2x^2)}$$

Virtual-photon flux

$$\Gamma = \frac{\alpha_{em}K}{2\pi^2 Q^2}\frac{E'}{E}\frac{1}{1-\epsilon}$$

Hand convention:

$$K = \nu - \frac{Q^2}{2M}$$

$$\frac{d^2\sigma}{d\Omega\, dE'} = \Gamma[\sigma_T(x,Q^2)+\epsilon\sigma_L(x,Q^2)]$$

Virtual-photon polarization parameter

$$\epsilon = \frac{4(1-y)-Q^2/E^2}{4(1-y)+2y^2+Q^2/E^2}$$

Define ratio **R** and re-parameterize cross section

$$R = \frac{\sigma_L}{\sigma_T}$$

$$\frac{d^2\sigma}{dx\,dQ^2} = \frac{4\pi\alpha_{em}^2}{Q^4}\frac{\boldsymbol{F_2}}{x}\times\left[\,1-y-\frac{Q^2}{4E^2}+\frac{y^2+Q^2/E^2}{2(1+\boldsymbol{R}(x,Q^2))}\,\right]$$

Kinematic Plane in x-Q^2

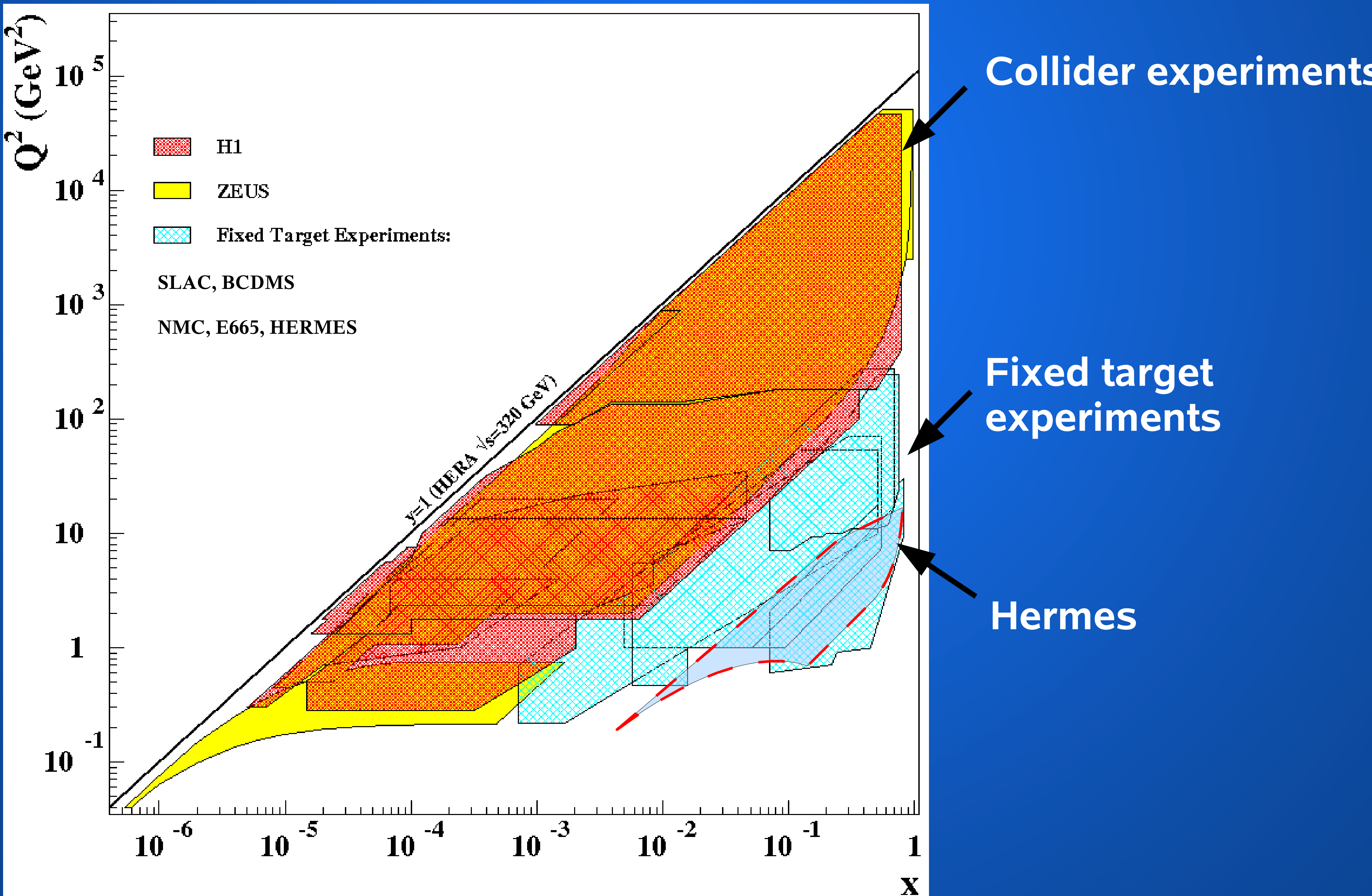

Why measuring *inclusive* *DIS cross sections* at Hermes?

World largest data set on deuteron

Hermes (1996-2005)	**30 M proton + 28 M deuteron**
	~450 pb^{-1} ~460 pb^{-1}
e.g.: compared to NMC	3 M proton + 6 M deuteron

$F_2^p, \; F_2^d$

World data fits
$\sigma^{p,d}, \; \sigma^d/\sigma^p$

Gottfried Sum
$\int \frac{dx}{x}(F_2^p - F_2^n)$

d_v / u_v

The HERMES Spectrometer

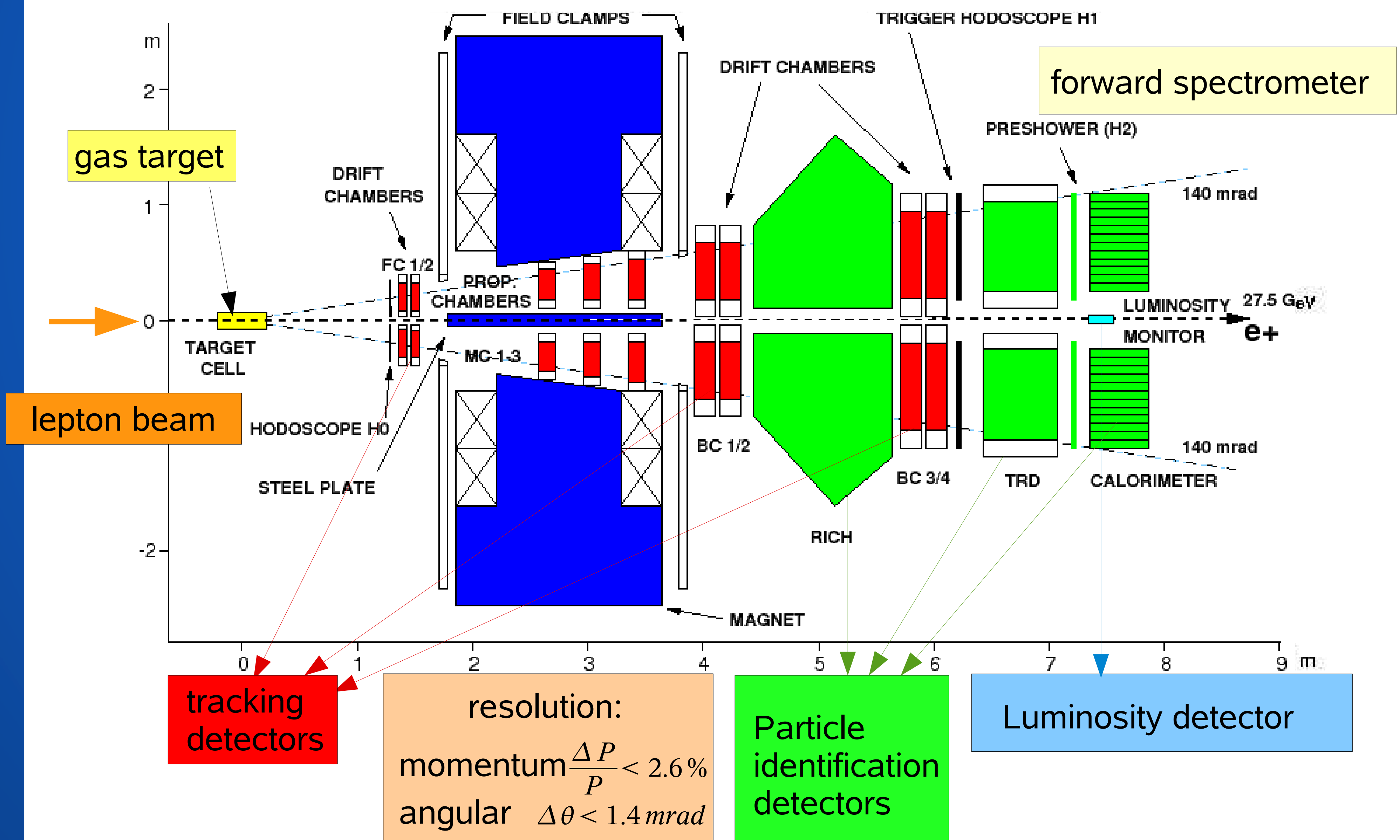

resolution:

momentum $\frac{\Delta P}{P} < 2.6\,\%$

angular $\Delta\theta < 1.4\, mrad$

Binning in x and Q^2

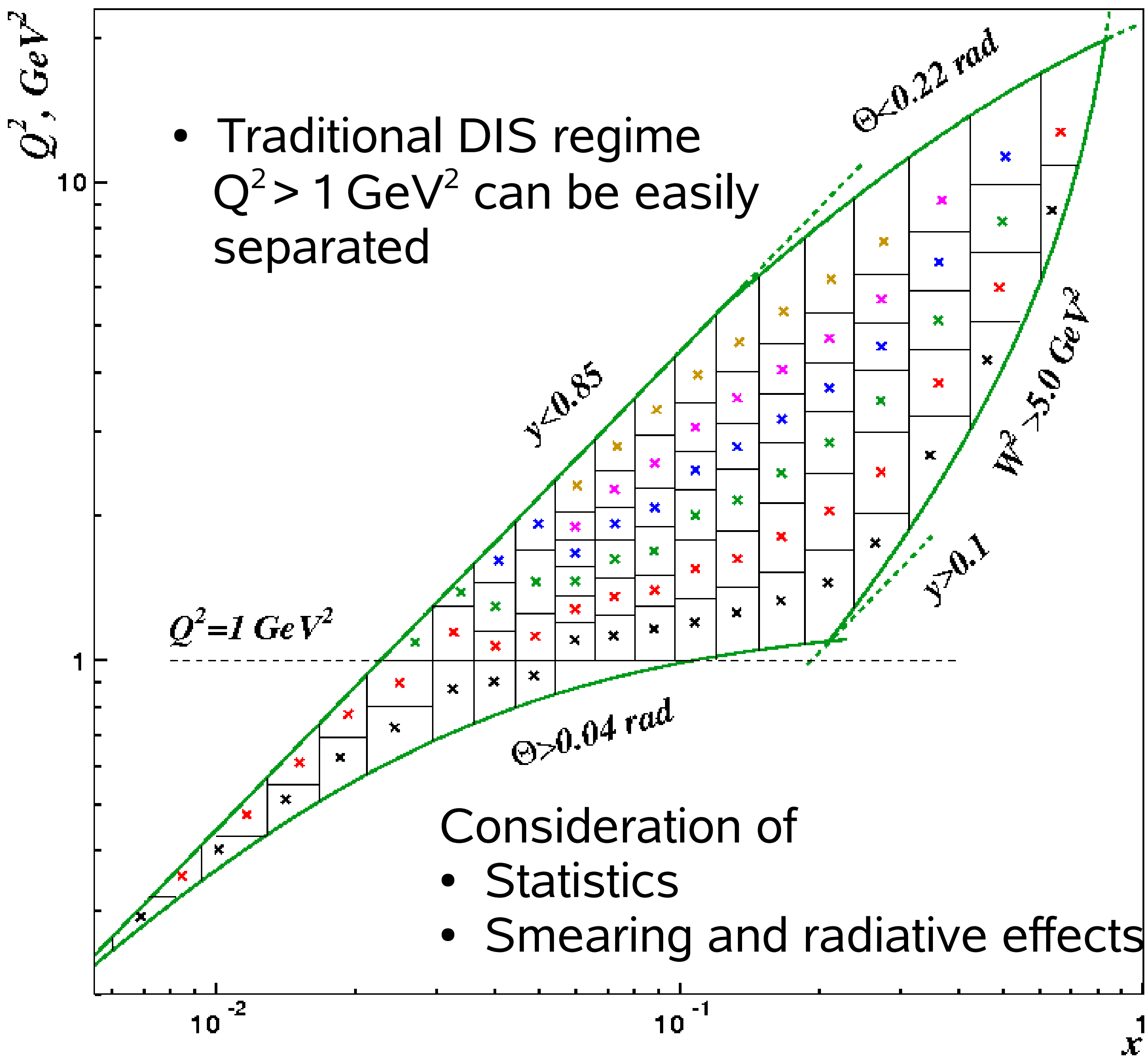

- Traditional DIS regime $Q^2 > 1\ GeV^2$ can be easily separated

Consideration of
- Statistics
- Smearing and radiative effects

kinematic region

- $0.006 < x < 0.9$
- $0.1 < y < 0.85$
- $0.2\ GeV^2 < Q^2 < 20\ GeV^2$
- $W^2 > 5\ GeV^2$
- $0.04\ rad < \Theta < 0.22\ rad$

binning

- 19 x bins
- up to 6 Q^2 bins
- Total: 81 bins

Extraction of cross sections

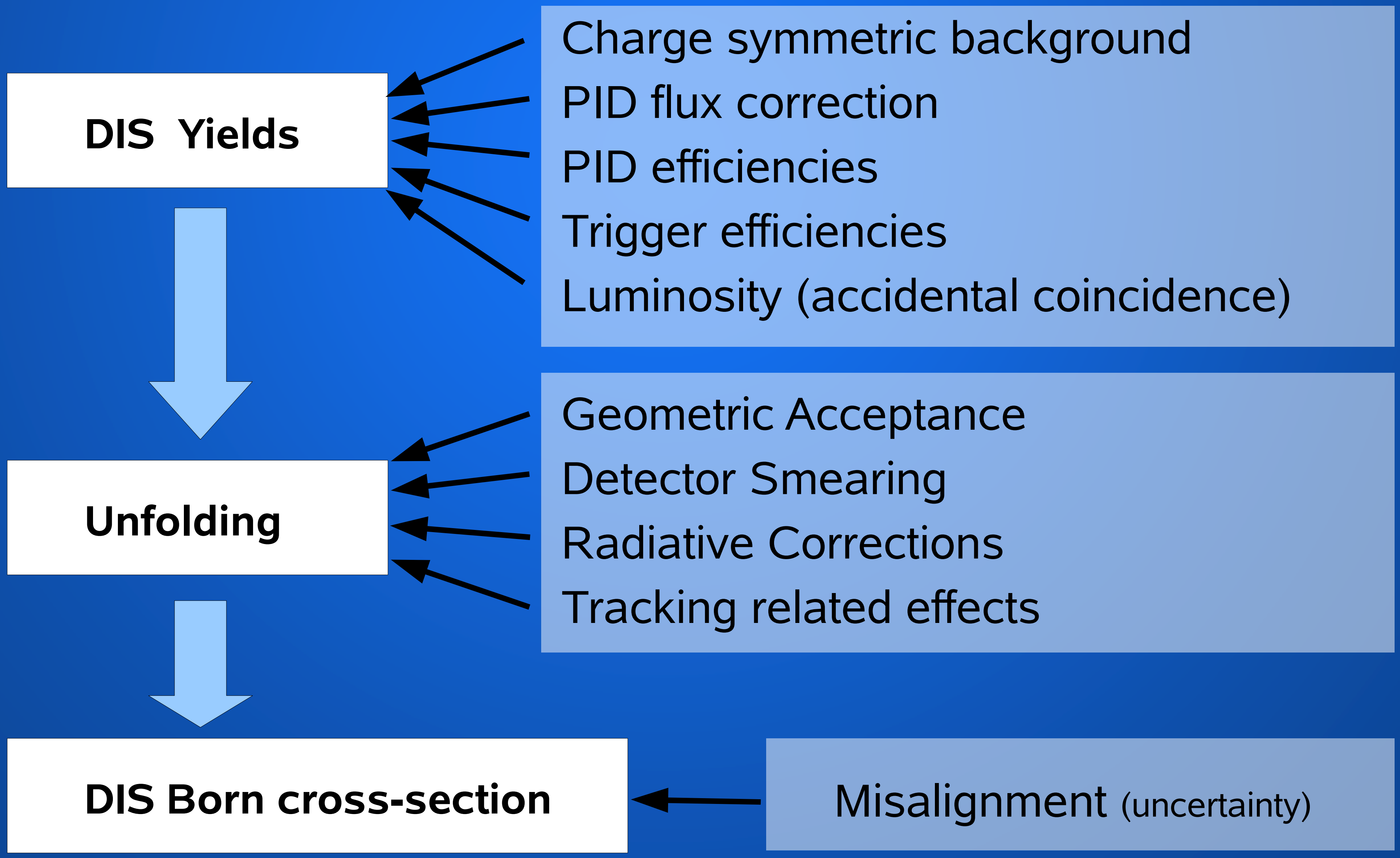

Luminosity

- Elastic reference process
- Interaction of beam with shell electrons
  - Electron Beam: Møller scattering $e^- e^- \rightarrow e^- e^-$
  - Positron Beam: Bhabha scattering $e^+ e^- \rightarrow e^+ e^-$, annihilation $e^+ e^- \rightarrow \gamma\gamma$
- Coincidence rate R_{RL} in Δt = 80ns time resolution window
- Luminosity "constants" C_{Lumi} convert coincidence rate into luminosity (pb^{-1})
- Uncertainties of ~ 3% - 8%. Acceptance of L. detector depends on e.g.
  - beam conditions
  - magnetic fields

Luminosity

Corr. for acciden-tal coincidence

Trigger life time

Time interval

$$L = \int_b \mathcal{L}\, dt = (R_{LR} - \Delta t \cdot R_L \cdot R_R) \cdot C_{Lumi} \frac{A}{Z} \cdot l \cdot \Delta b$$

Coincidence rate

Luminosity constant

A: nucleons
Z: shell electrons

$$\sigma_{DIS} = \frac{N_{DIS}}{\int \mathcal{L}\, dt}$$

DIS yield

Particle identification

TRD

Cherenkov (RICH)

Preshower

Calorimeter

conditional probabilities
for particle hypotheses

$$PID \;=\; PID_{det} - \log_{10} \Phi$$

$$\Phi = \frac{\phi_h}{\phi_l} = \frac{P(H_h | p, \theta)}{P(H_l | p, \theta)}$$

relative contributions
hadrons and leptons

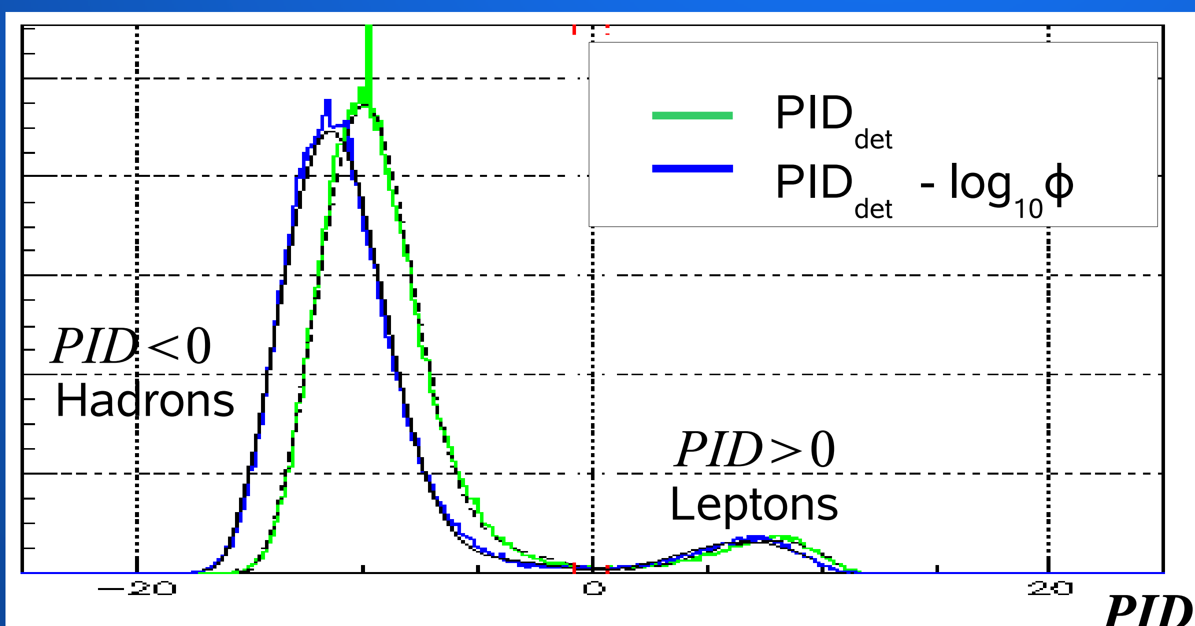

PID efficiency and contamination

Lepton sample identified by: $PID > PID_l$ with $PID_l = 0$

- high efficiencies and small contaminations at same time

Contamination of lepton sample

C = Fractional contribution of hadrons in the lepton sample

$$\frac{\int_{PID_l} dPID\, N_h}{\int_{PID_l} dPID (N_l + N_h)}$$

Efficiency lepton identification

ε = Fraction of leptons selected with PID>0

$$\frac{\int_{PID_l} dPID\, N_l}{\int dPID\, N_l}$$

Correction:

$$N_{cor} = N_{unc} \cdot \frac{1 - C(PID_l)}{\varepsilon(PID_l)}$$

Due to correlations between PID detectors, assign uncertainty of full size of correction

PID efficiency and contamination

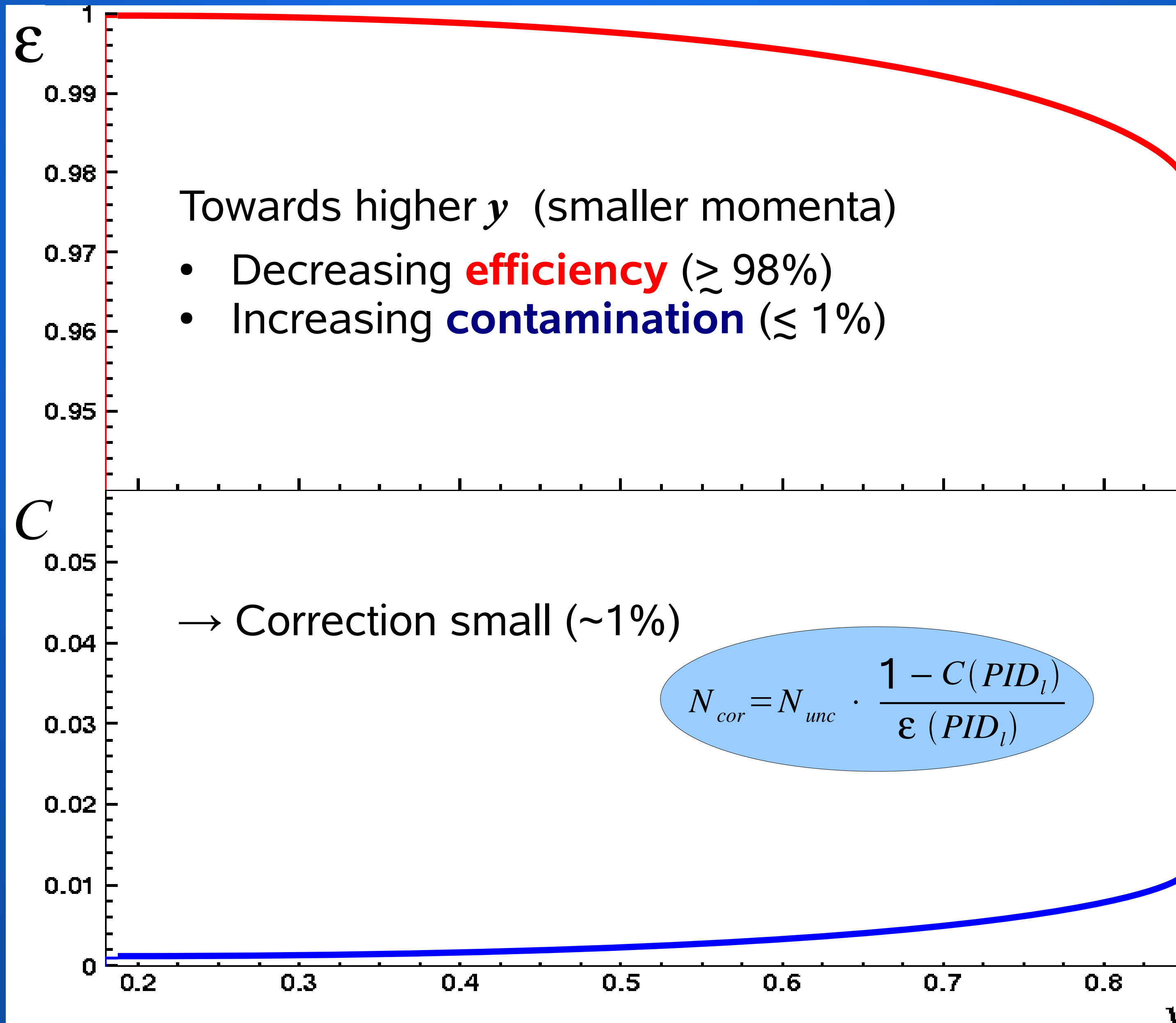

Trigger efficiencies

- Trigger = combination of fast signals
- Select events of specific interest

DIS trigger (tr21): H0 + H1 + H2 + Calorimeter

H o d o s c o p e s (H0, H1, H2)

$$\varepsilon(tr21) = \varepsilon(H0) \cdot \varepsilon(H1) \cdot \varepsilon(H2) \cdot \varepsilon(CA)$$

- Trigger efficiencies for each year. Depend on time, momentum, angle.

E.g. 2000:

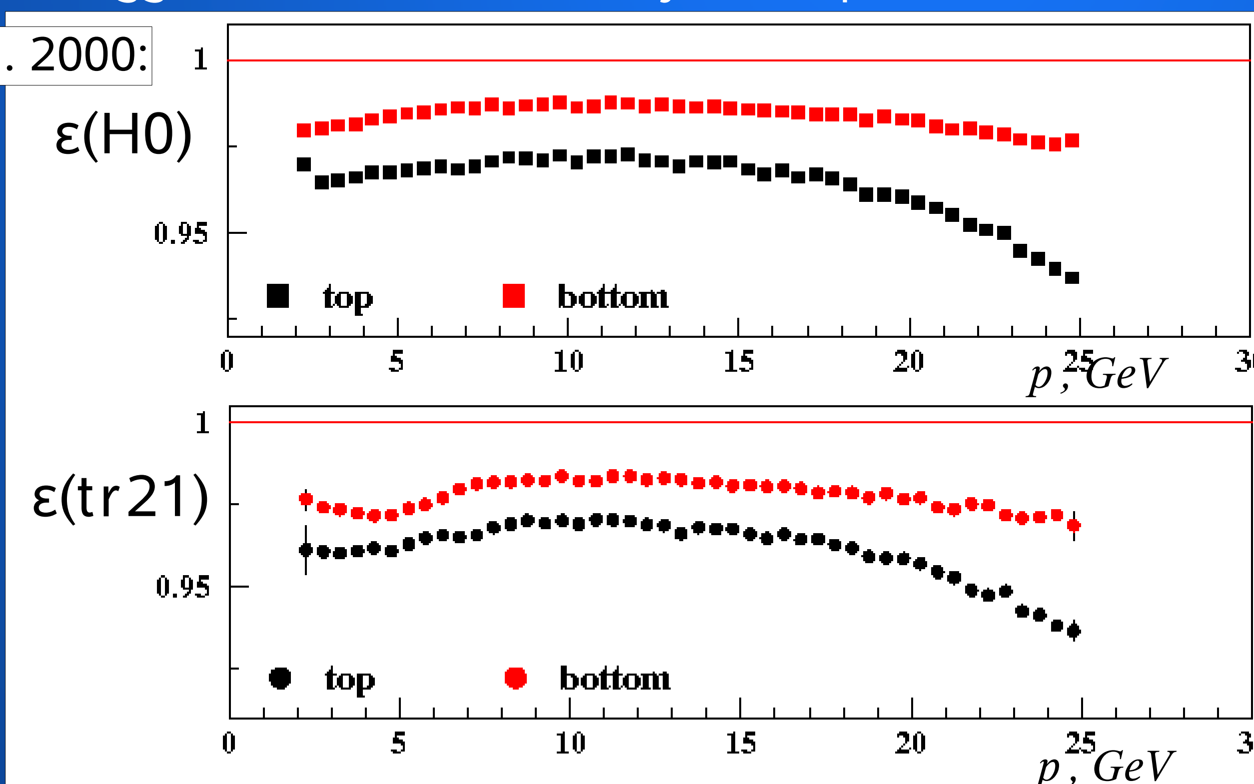

- ε(H1), ε(H2), ε(CA) >99%
- ε(H0) ~ 97% low!
- Different in top, bot.

- **H0 inefficiencies dominate trigger 21 inefficiency**
  → contrib. to top-bot-asym.

- **Correction** by counting each event with inverse of efficiencies

$$w = \frac{1}{\epsilon}$$

QED radiative effects

Feynman diagrams of processes contributing to radiative corrections:

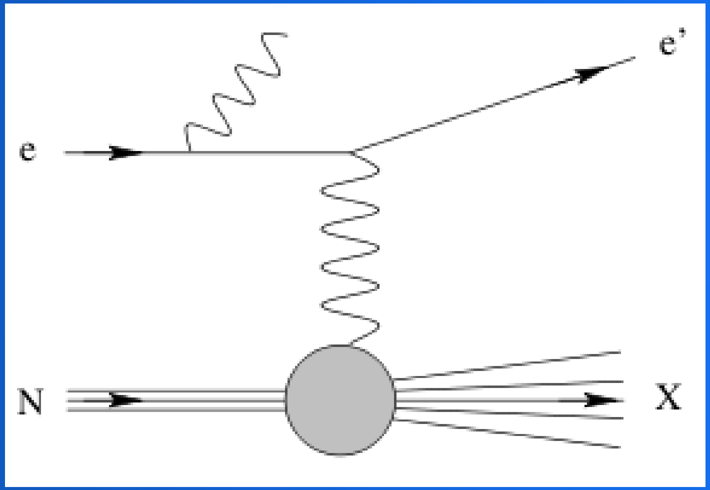

initial state radiation

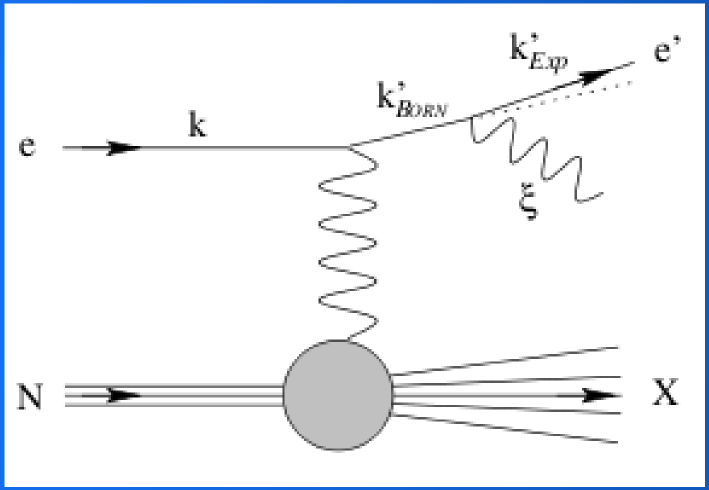

final state radiation

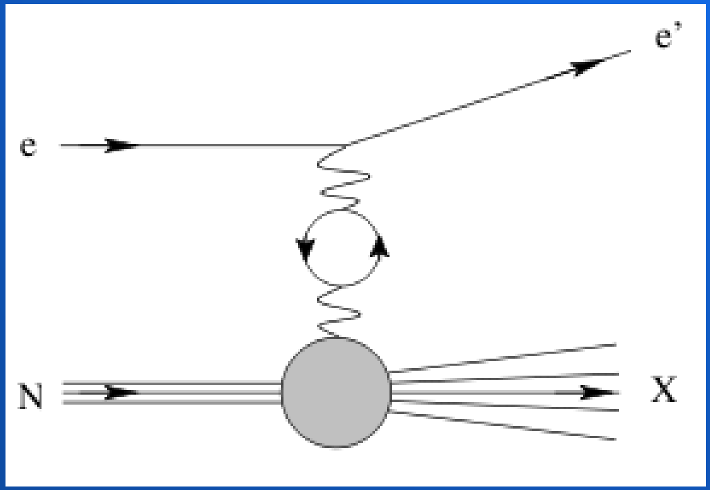

vacuum polarization

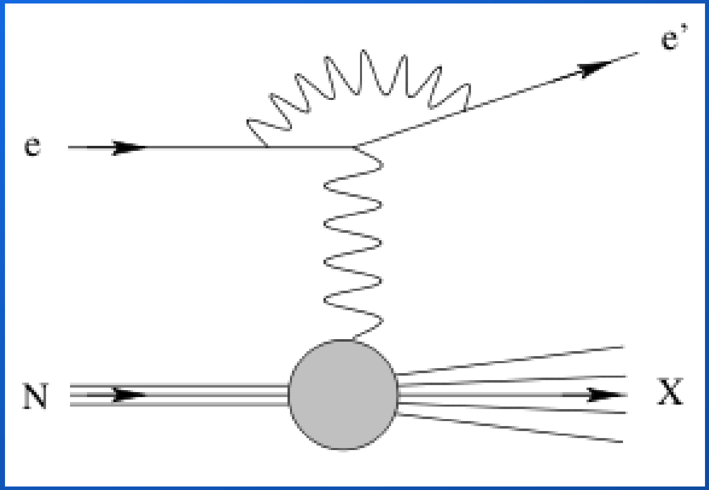

vertex correction

Migration matrix

Binning in *x* — Binning in *x*-Q^2

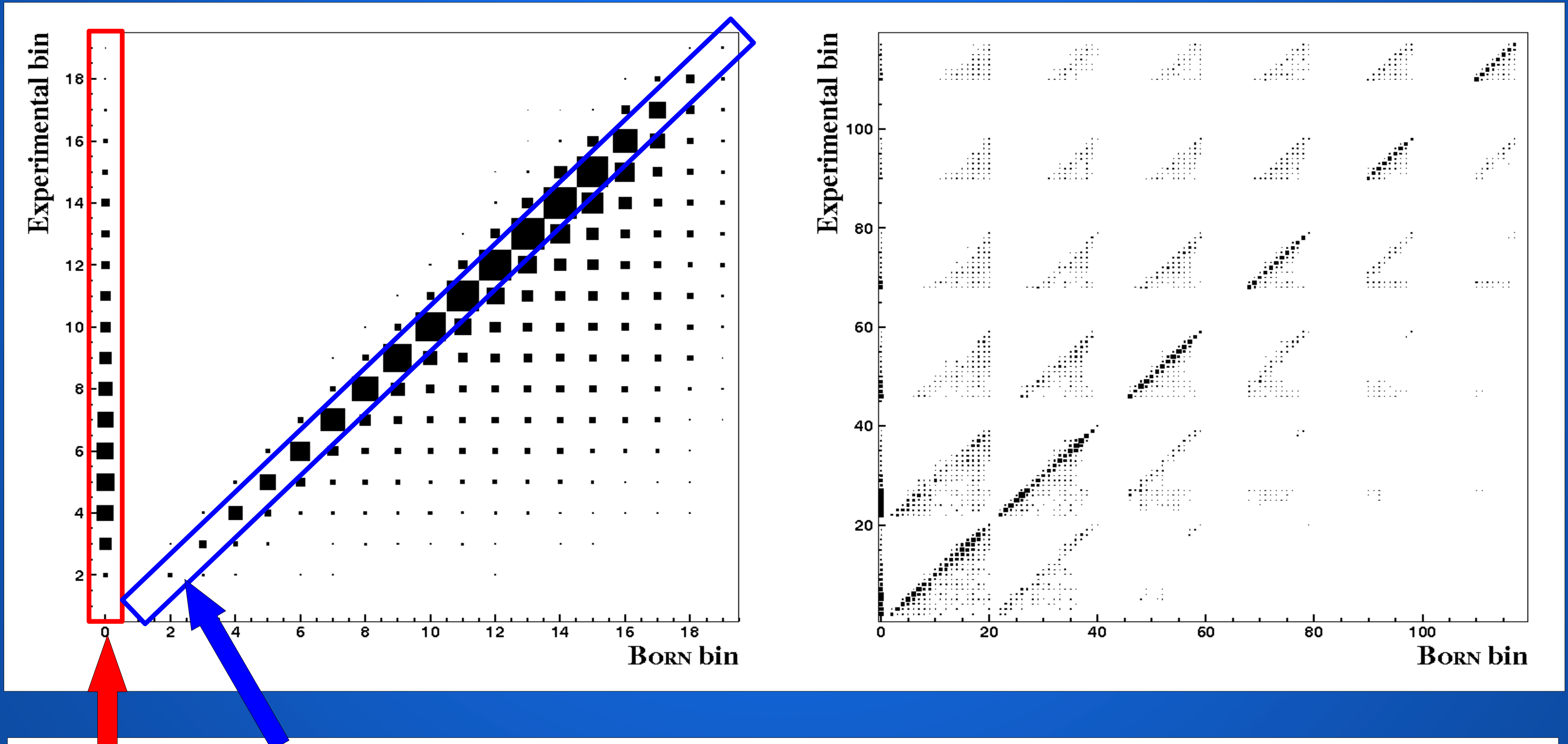

Diagonal elements on migration matrix, measured bin = Born level bin

Migration into acceptance from outside n(i,0), i>0

Unfolding of kinematic bin migration

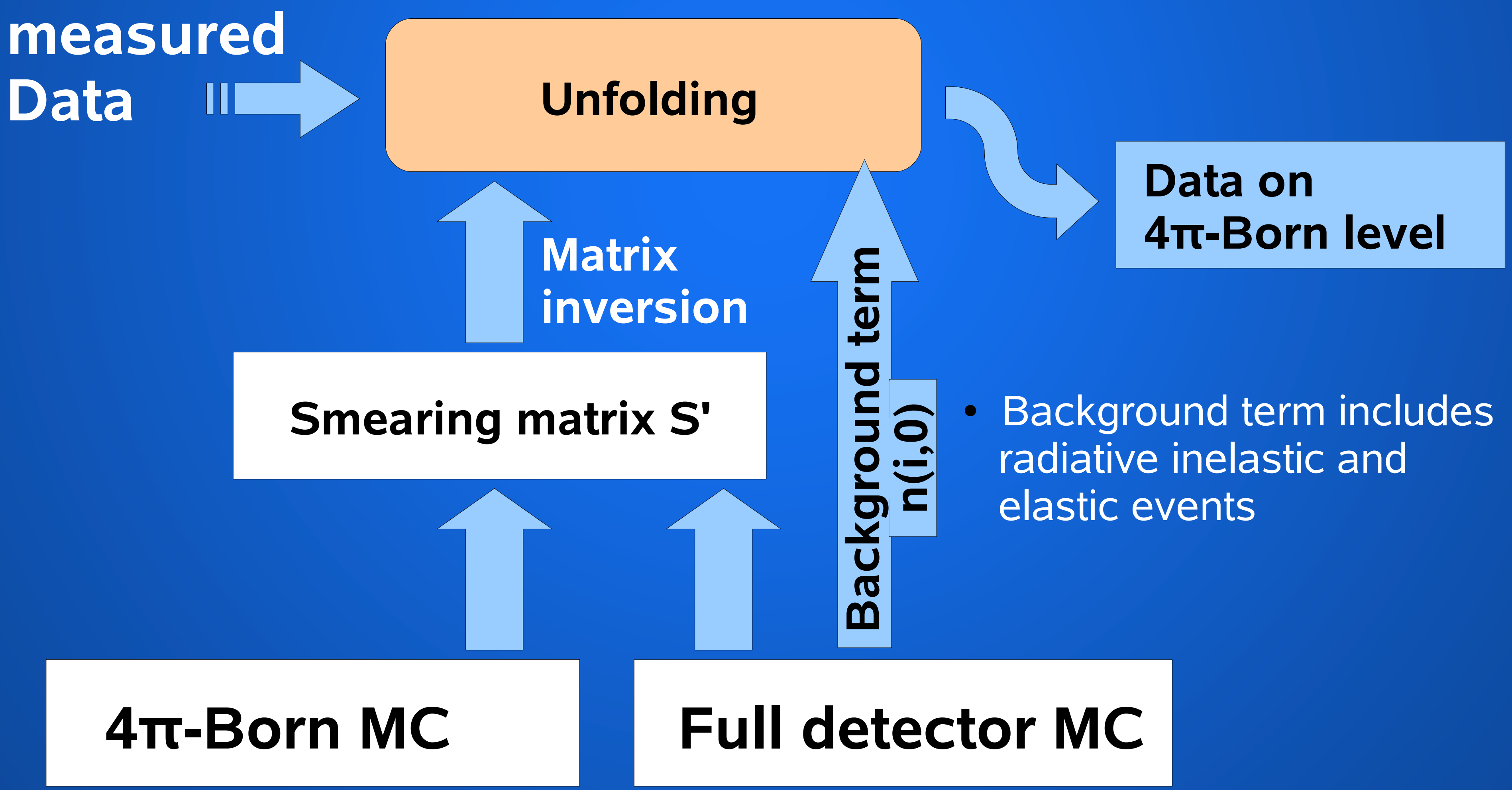

- Background term includes radiative inelastic and elastic events

Simulation of true cross section
No radiative effects
No tracking

Detector material (GEANT4)
Radiative effects
Tracking

Bethe-Heitler Cross section

Bethe-Heitler: Radiation of real photons associated with elastic interaction of charged particle with the electromagnetic nuclear field

Due to photon radiation, the apparent kinematic variables of Bethe-Heitler events can be indistinguishable from DIS events. → Background to DIS.

Three cases

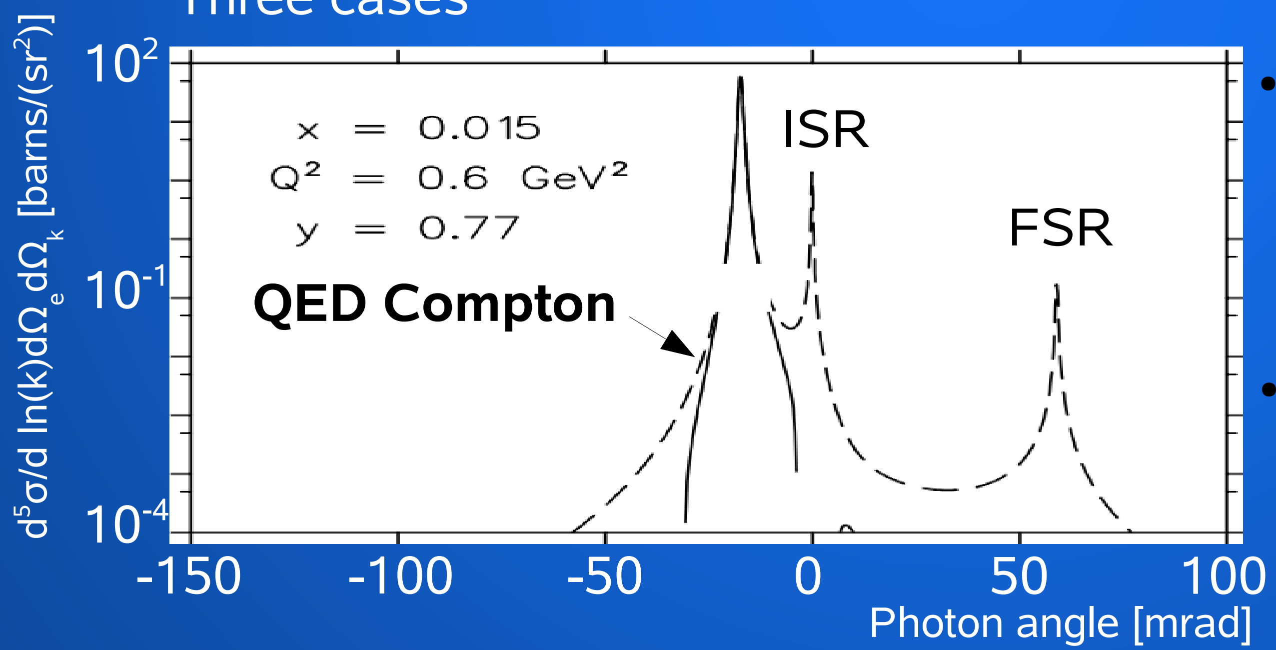

- Initial state radiation (ISR) photon radiation along incoming lepton (lost in the beam pipe)
- Final state radiation (FSR) photon radiation along outgoing lepton

- **QED Compton** photon radiation at finite angles

$$(1-y)\sin\theta_{e'} = y \sin\theta_{\gamma}$$

→ high probability to **hit detector frames**

Bethe-Heitler efficiencies

- Bethe-Heitler efficiencies **extracted from MC** for proton and deuteron

Proton

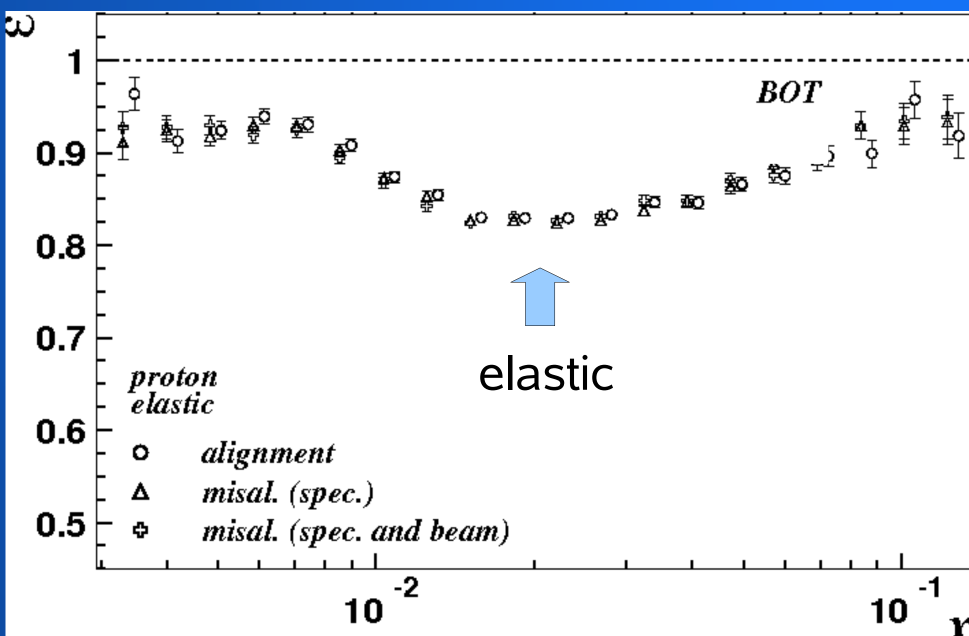

Deuteron

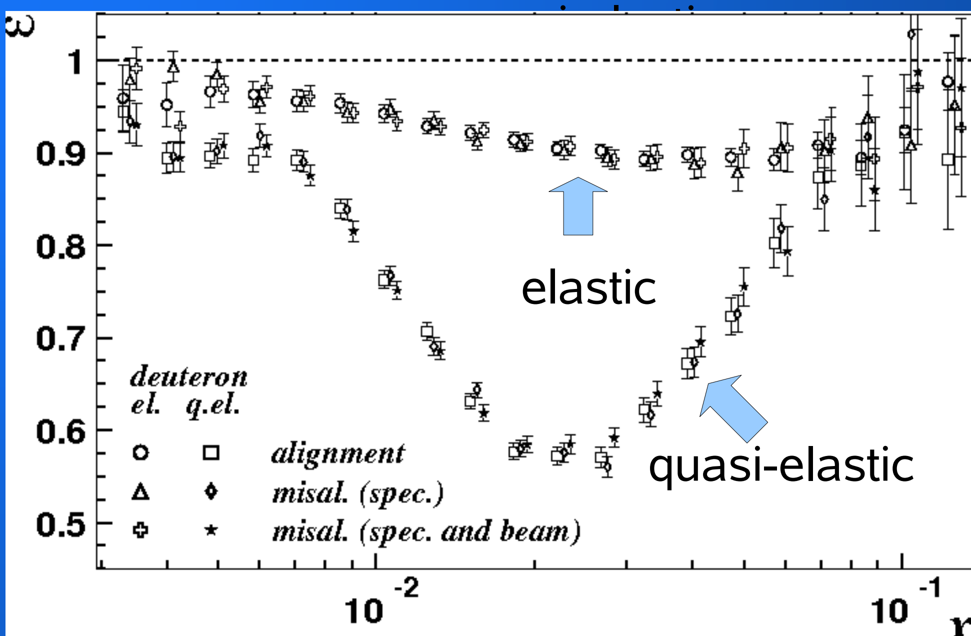

- Bethe-Heitler efficiencies are relevant for unfolding

Misalignment

Perfect alignment | **Misalignment of the spectrometer** | **Misal. of beam and spectrometer**

- **Ideal situation**: Perfect alignment of beam and spectrometer
- In practice:
  - Top and bottom parts of **spectrometer** displaced
  - **Beam position** differs from nominal position

- Beam misalignment measured by beam monitors
- Analysis of tracks in the top and bottom halves provides information about misalignment of spectrometer

Misalignment of

Beam (1998, 2000)

	e^-	e^+
X-slope (mrad)	-0.014	-0.035
Y-slope (mrad)	-1.200	-0.420
X-offset (cm)	0.015	0.017
Y-offset (cm)	0.090	0.160

Spectrometer

	top	bot
X-slope (mrad)	0.44	0.24
Y-slope (mrad)	-1.2	0.02
X-offset (cm)	-0.09	-0.11
Y-offset (cm)	-0.01	0.11

Misalignment

Simulation of misalignment in MC:

$$\frac{\sigma_{misaligned}}{\sigma_{aligned}}(top)$$

$$\frac{\sigma_{misaligned}}{\sigma_{aligned}}(bot)$$

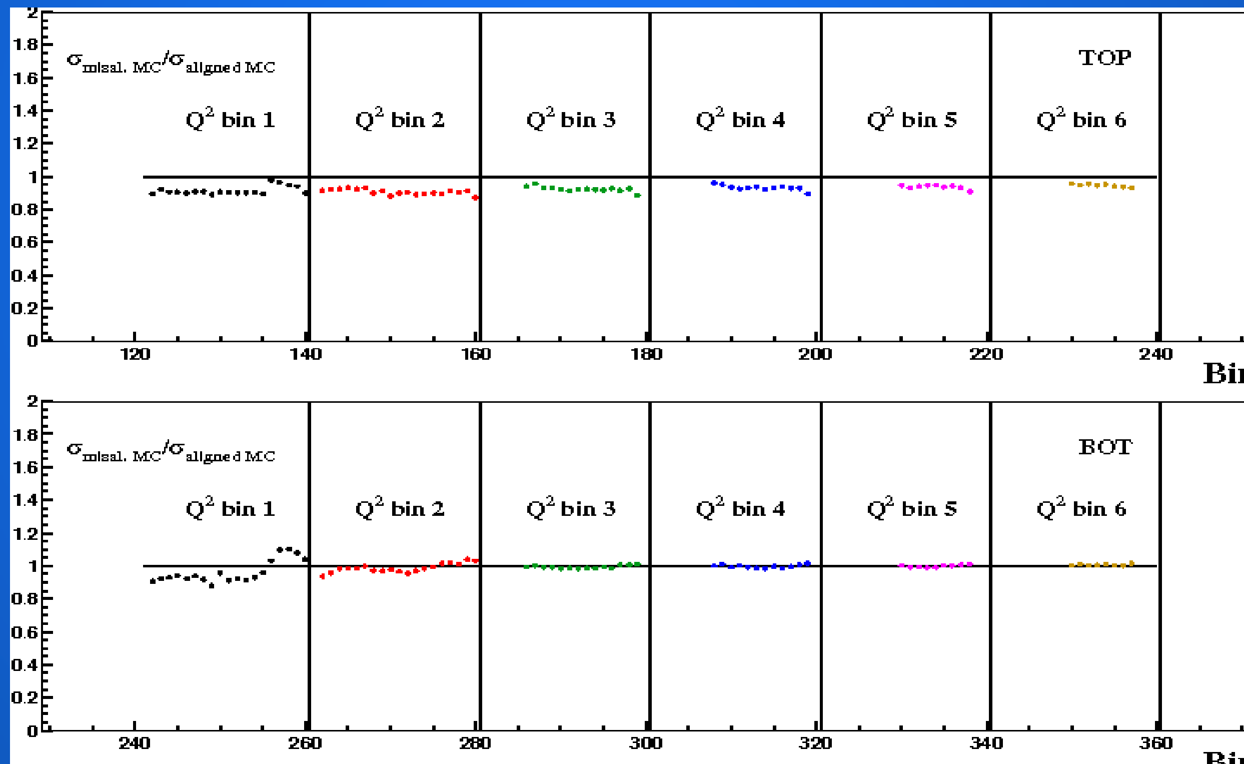

- “Misalignment ratio”: Effect of misalignment is in the order of 7%.
- No correction for misalignment but assignment of uncertainty: $\left| \frac{\sigma_{misaligned}}{\sigma_{aligned}} - 1 \right|$
- Unfolding of the misalignment ratio to Born level

Systematic uncertainties on σ^p, σ^d

- Which systematic uncertainties are assigned.

δ_{PID} : PID misidentification
typically ~ 1%

$\delta_{rad.}$: Unc. of BH efficiencies due to misalignment
$\lesssim$ 1%

δ_{mis} : Misalignment effect on DIS events
~ 7%

δ_{nor} : Overall normalization unc.: Luminosity
δ^p_{nor} = 6.4 % δ^d_{nor} = 6.6 %

Fit to world data of proton DIS cross-sections

Fit with the following features

- Based on the *ALLM functional from* for the γp cross section
  - Regge-motivated, phenomenological approach
  - allows very good description of measured regions
  - constructed so that photoproduction data at $Q^2=0$ can be included

NEW
- *Normalization uncertainties* are considered by an accurate method involving a penalty term in χ^2.

NEW
- *Fit uncertainties* are determined. Covariance matrix provided for the first time.

NEW
- *Self-consistent* with respect to the use of $R=\frac{\sigma_L}{\sigma_T}$

NEW
- This fit includes *newer data* and covers ***2821 data points***. This is more than twice as much as used in ALLM97 (1356 data points).

- Fit results available in F0RTRAN routine:
  http://www-hermes.desy.de/users/dgabbert/SIGMATOT_PARAM.tgz

Fit to world data of proton DIS cross-sections

- The DIS cross-section in the 1-photon exchange approximation:

$$\frac{d^2\sigma}{dx\, dQ^2} = \frac{4\pi\alpha_{em}^2}{Q^4} \frac{F_2}{x} \times \left[1 - y - \frac{Q^2}{4E^2} + \frac{y^2 + Q^2/E^2}{2(1+R(x,Q^2))} \right]$$

  for all data sets

- F_2 can be related to the full cross-section $\sigma = \sigma_L + \sigma_T$

$$\sigma_{L+T}(\gamma p) = \frac{4\pi\alpha}{Q^2(1-x)} \frac{Q^2 + 4M^2x^2}{Q^2} F_2(W^2, Q^2)$$

- Consistent treatment of R

Fit to world data of proton DIS cross-sections

- The DIS cross-section in the 1-photon exchange approximation:

$$\frac{d^2\sigma}{dx\, dQ^2} = \frac{4\pi\alpha_{em}^2}{Q^4}\frac{F_2}{x} \times \left[1 - y - \frac{Q^2}{4E^2} + \frac{y^2 + Q^2/E^2}{2(1+R(x,Q^2))} \right]$$

for all data sets

- F_2 can be related to the full cross-section $\sigma = \sigma_L + \sigma_T$

$$\sigma_{L+T}(\gamma p) = \frac{4\pi\alpha}{Q^2(1-x)}\frac{Q^2 + 4M^2x^2}{Q^2} F_2(W^2, Q^2)$$

- Consistent treatment of R

Central values of the two common parameterizations

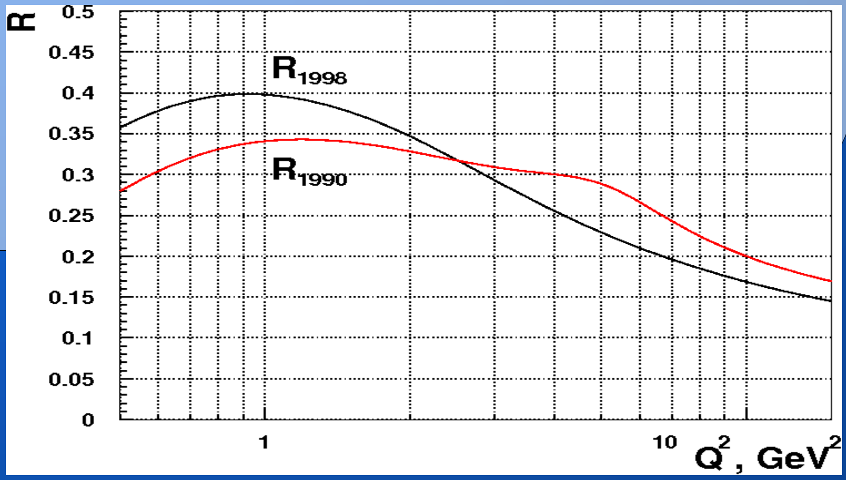

X^2 - Minimization

X^2 - Minimization

$$X^2 = \sum_{i}^{n_{max}} \frac{(\sigma_i^{\exp} - \sigma_i^{th})^2}{\delta^2_{i\ sta} + \delta^2_{i\ sys}}$$

General definition

X^2 - Minimization

X^2 - Minimization

$$X^2 = \underbrace{\sum_{i}^{n_{max}} \frac{(\sigma_i^{\exp} - \sigma_i^{th}/(1+\nu_k \delta_{k(i)}^{norm}))^2}{\delta_{i\ sta}^2 + \delta_{i\ sys}^2}}_{\text{data points}} + \underbrace{\sum_k \nu_k^2}_{\text{data sets}}$$

- Introduce normalization parameters ν_k considered to be normal distributed – implemented by a penalty term.
- The normalization parameters ν_k defined in order to perform a re-normalization according to normalization error $\delta_{k(i)}^{norm}$.
- The analytic solution of ν_k for a fixed set of model parameters can be obtained from $d X^2 / d \nu_k = 0$, since ν_k are independent.

Error propagation

Error propagation

$$V[\sigma_{L+T}(\boldsymbol{p}, x, Q^2)] = \sum_{i,j} cov_{i,j}^{p} \frac{d\sigma_{L+T}(\boldsymbol{p}, x, Q^2)}{dp_i} \frac{d\sigma_{L+T}(\boldsymbol{p}, x, Q^2)}{dp_j}$$

V	variance
$\boldsymbol{p}$	parameter vector
$cov_{i,j}^{p}$	covariance matrix for $\boldsymbol{p}$

F_2 fit results (GD08)

Nr.	Exp	n	χ^2/n	δ_k^{nor}	ν_k
1.	SLAC-E49a	98	0.51	2.1	0.06
2.	SLAC-E49b	187	1.15	2.1	-0.28
3.	SLAC-E61	25	0.24	2.1	0.01
4.	SLAC-E87	94	0.68	2.1	0.07
5.	SLAC-E89a	72	1.06	2.1	1.31
6.	SLAC-E89b	98	1.01	2.1	0.17
7.	NMC 90 GeV	73	0.77	2.0	-0.37
8.	NMC 120 GeV	65	1.54	2.0	0.14
9.	NMC 200 GeV	75	1.13	2.0	-0.09
10.	NMC 280 GeV	79	0.94	2.0	-0.24
11.	E665	91	1.04	1.8	0.67
12.	BCDMS 100 GeV	58	1.13	3.0	-1.20
13.	BCDMS 120 GeV	62	0.73	3.0	0.03
14.	BCDMS 200 GeV	57	1.32	3.0	-1.09
15.	BCDMS 280 GeV	52	1.12	3.0	-1.03
16.	H1 94 a	37	0.35	3.9	0.05
17.	H1 94 b	156	0.63	1.5	1.13
18.	H1 SVX	44	0.49	3.0	-3.02
19.	ZEUS 94	188	1.15	2.0	1.66
20.	ZEUS BPC	34	0.40	2.4	-1.28
21.	ZEUS SVX	36	0.76	3.0	-1.00
24.	ZEUS 9697	242	0.75	2.0	0.09
25.	ZEUS 97	70	0.97	2.0	-2.23
26.	H1 99 00	147	1.01	1.5	-1.08
27.	H1 98 99	126	1.37	1.8	-1.38
28.	H1 94 97	130	0.79	1.5	-1.46
29.	H1 96 97 a	67	1.05	1.7	1.77
30.	H1 96 97 b	80	0.82	1.7	2.02
31.	**this analysis, HERMES**	**81**	**0.40**	**6.4**	**0.67**

Total: $\chi/n = 0.93$

F_2 fit results (GD08)

Nr.	Exp	n	χ^2/n	δ_k^{nor}	ν_k
1.	SLAC-E49a	98	0.51	2.1	0.06
2.	SLAC-E49b	187	1.15	2.1	-0.28
3.	SLAC-E61	25	0.24	2.1	0.01
4.	SLAC-E87	94	0.68	2.1	0.07
5.	SLAC-E89a	72	1.06	2.1	1.31
6.	SLAC-E89b	98	1.01	2.1	0.17
7.	NMC 90 GeV	73	0.77	2.0	-0.37
8.	NMC 120 GeV	65	1.54	2.0	0.14
9.	NMC 200 GeV	75	1.13	2.0	-0.09
10.	NMC 280 GeV	79	0.94	2.0	-0.24
11.	E665	91	1.04	1.8	0.67
12.	BCDMS 100 GeV	58	1.13	3.0	-1.20
13.	BCDMS 120 GeV	62	0.73	3.0	0.03
14.	BCDMS 200 GeV	57	1.32	3.0	-1.09
15.	BCDMS 280 GeV	52	1.12	3.0	-1.03
16.	H1 94 a				0.05
17.	H1 94 b				1.13
18.	H1 SVX				-3.02
19.	ZEUS 9				1.66
20.	ZEUS B				-1.28
21.	ZEUS S				-1.00
24.	ZEUS 9	[illegible]	[illegible]	[illegible]	0.09
25.	ZEUS 97	70	0.97	2.0	-2.23
26.	H1 99 00	147	1.01	1.5	-1.08
27.	H1 98 99	126	1.37	1.8	-1.38
28.	H1 94 97	130	.79	1.5	-1.46
29.	H1 96 97 a	67	05	1.7	1.77
30.	H1 96 97 b	80	0.82	1.7	2.02
31.	**this analysis, HERMES**	**81**	**0.40**	**6.4**	**0.67**

Low value of χ^2/n reflects
conservative assignment of uncertainties:
misalignment, overall normalization

Total: $\chi/n = 0.93$

F_2 fit results (GD08)

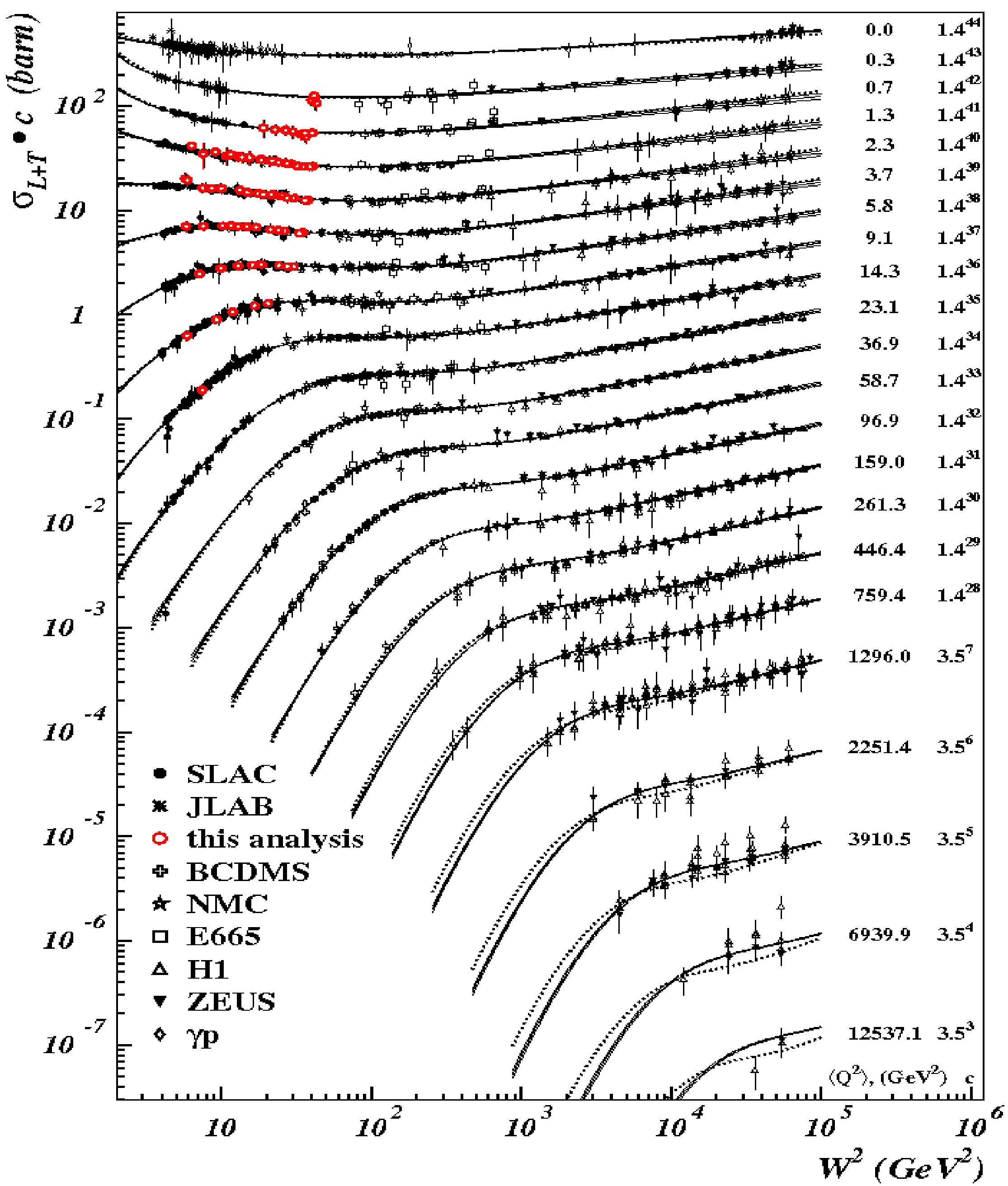

Results on F_2^p

Proton

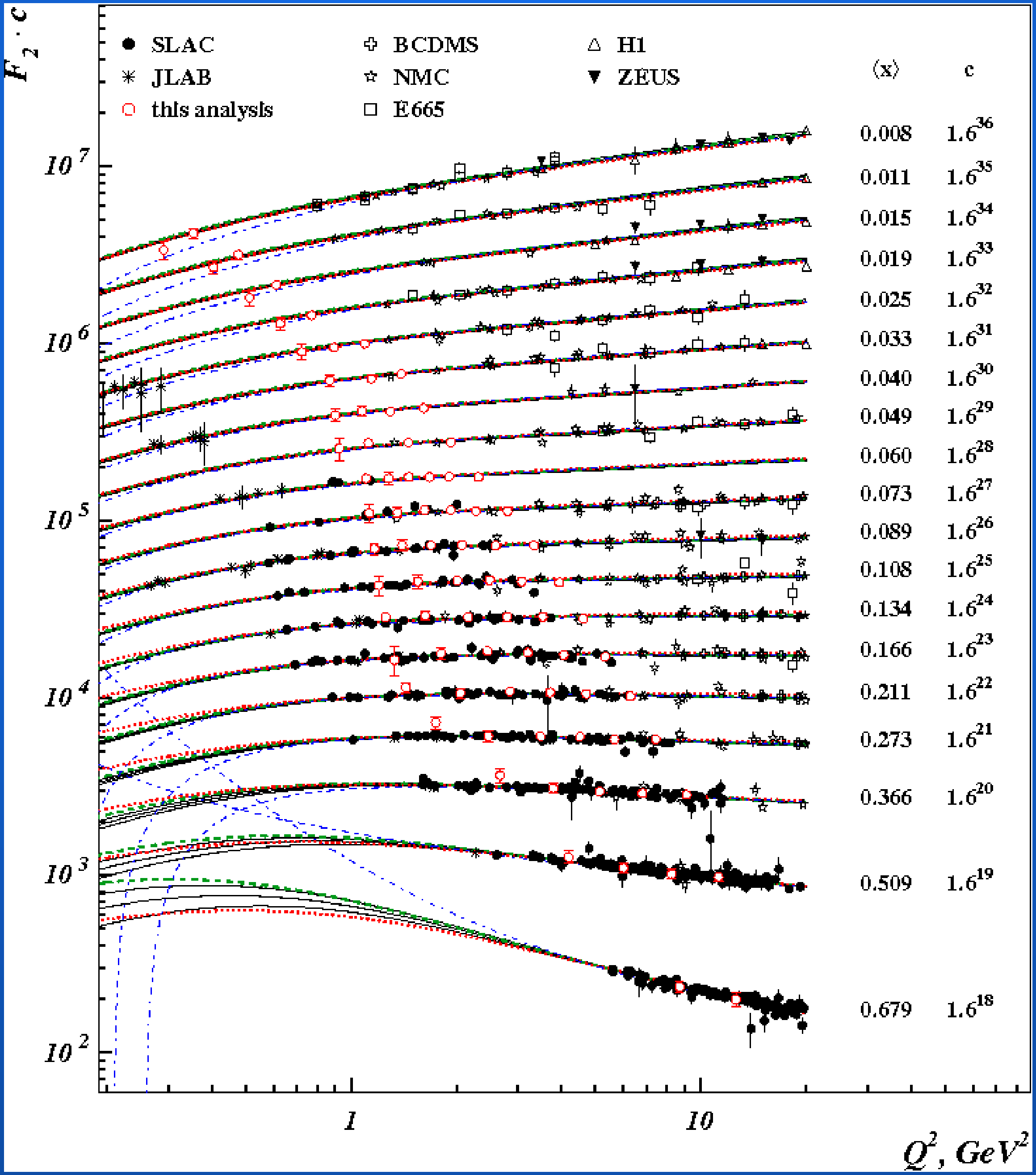

Results on F_2^p

Proton

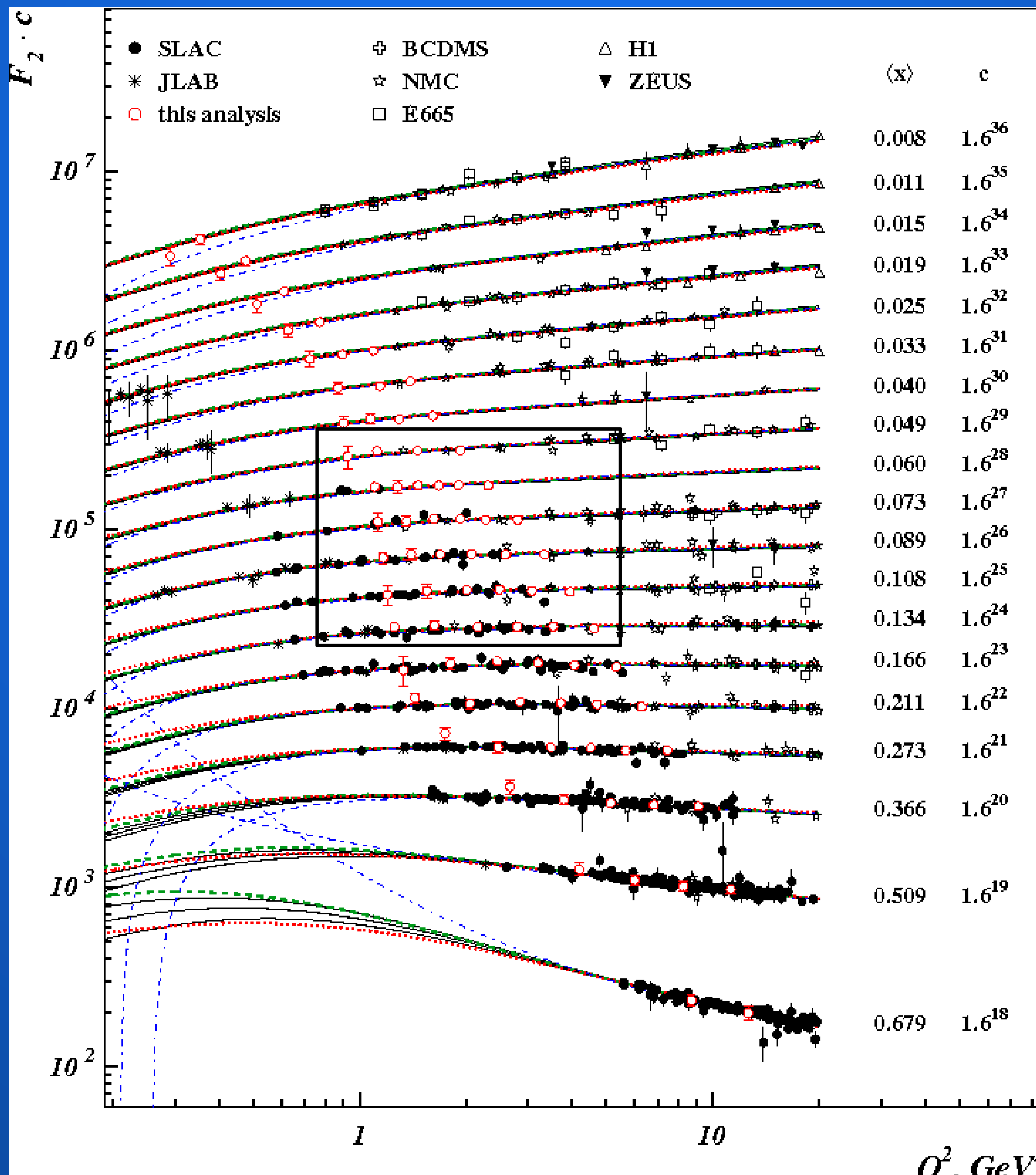

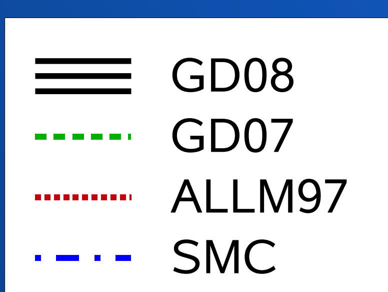

Results on F_2^p

Proton

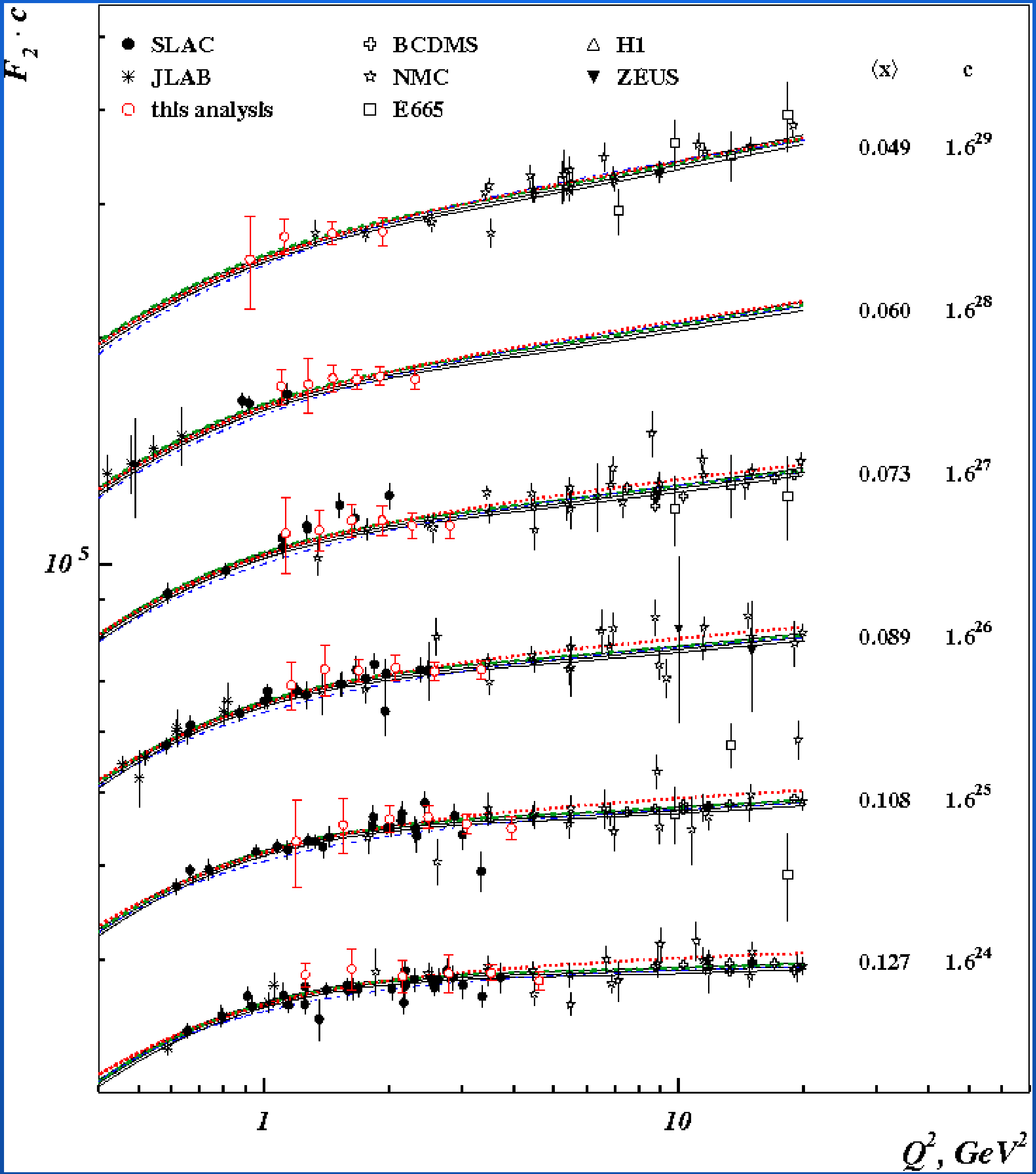

Results on F_2^d

Deuteron

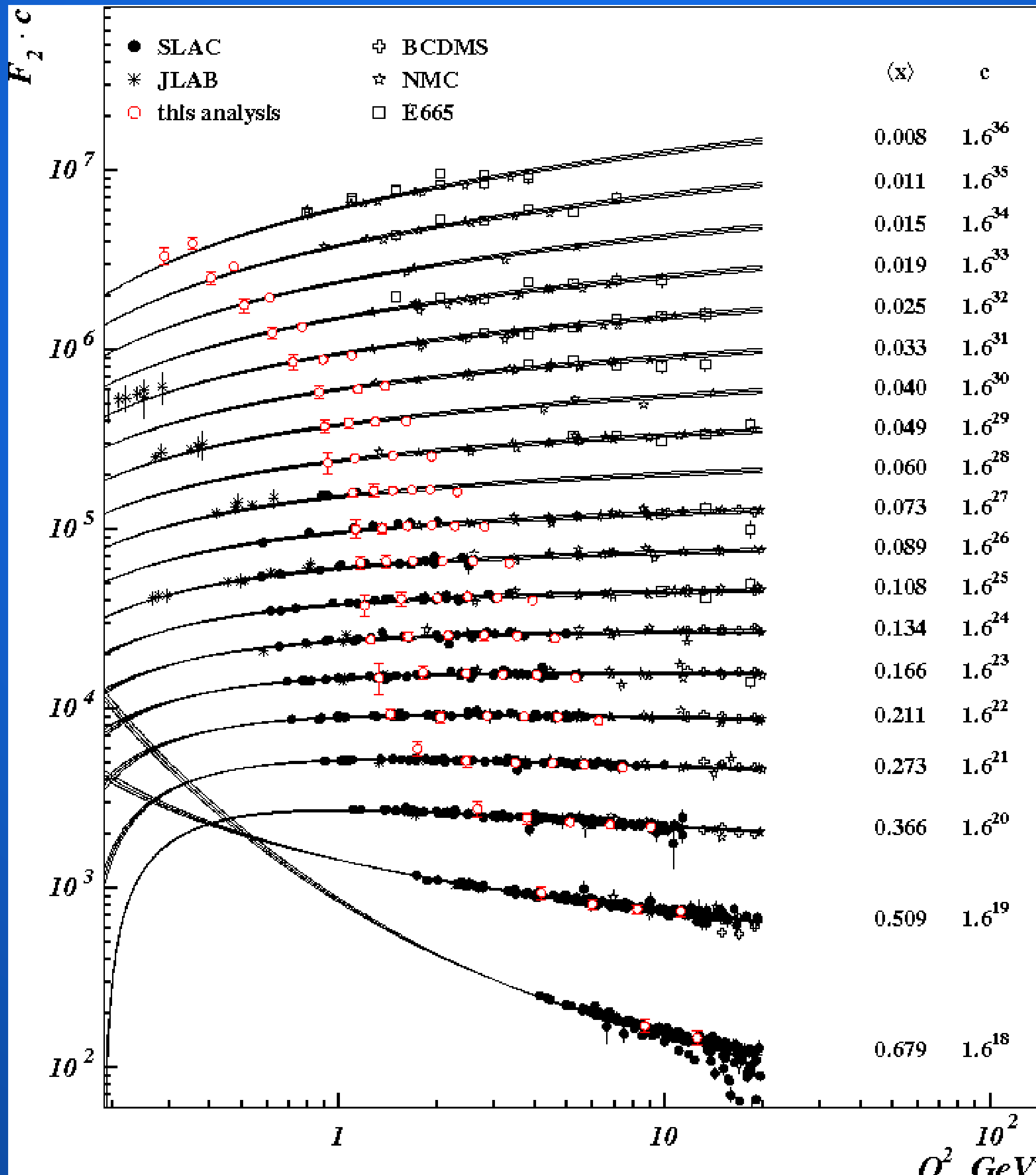

SMC

Results on F_2^d

Deuteron

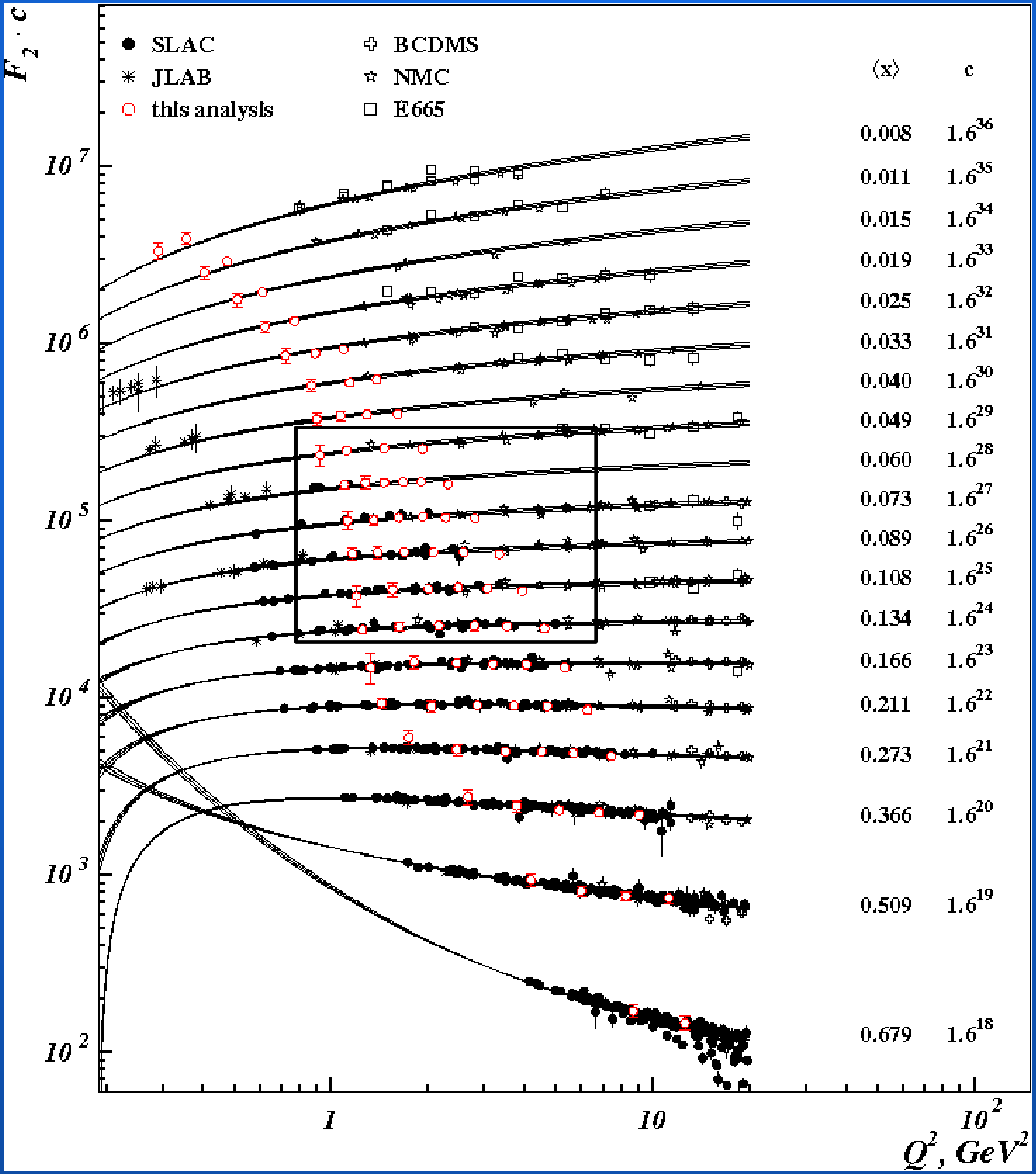

SMC

Results on F_2^d

Deuteron

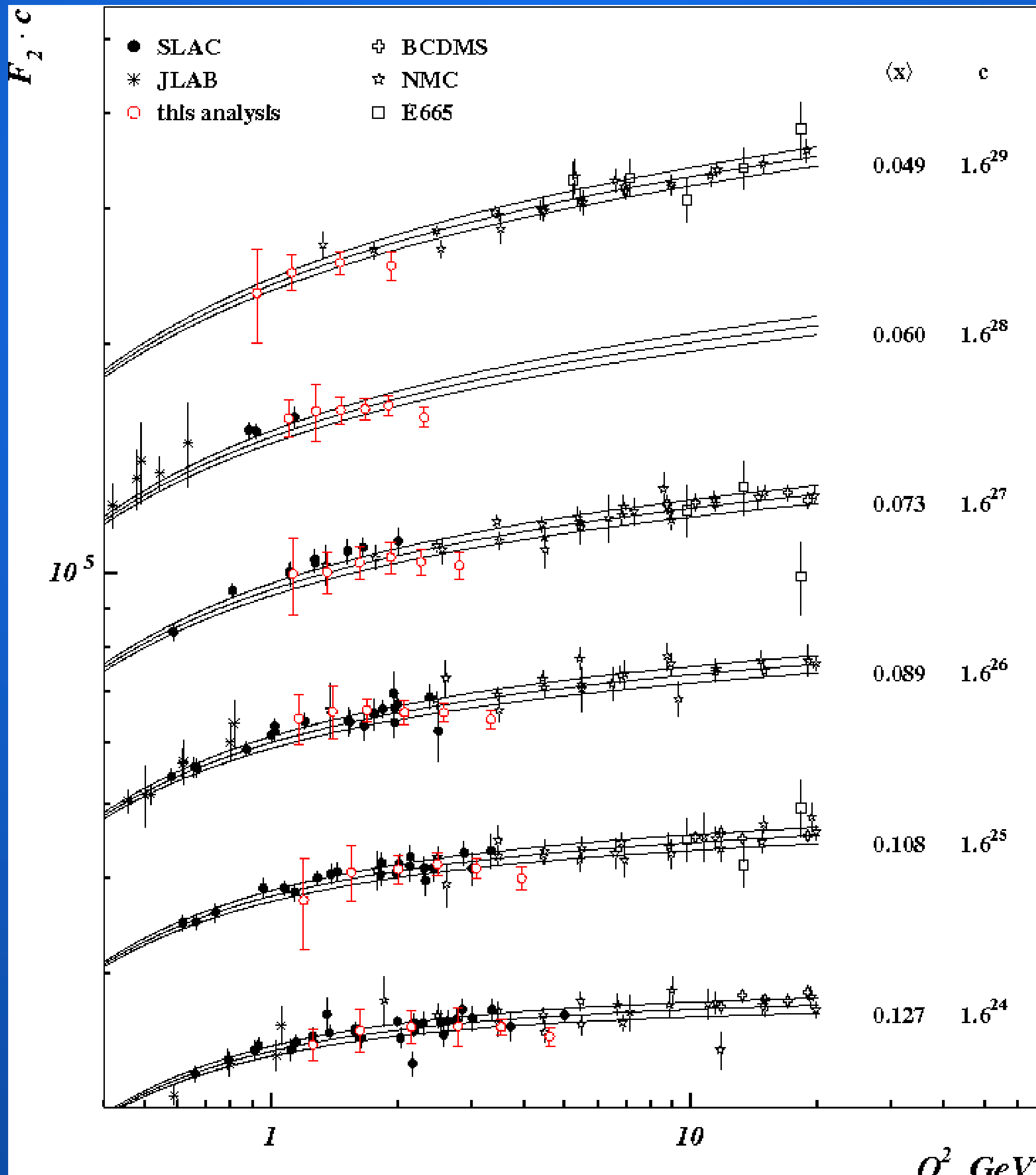

SMC

Why measuring *inclusive* *DIS cross sections* at Hermes?

hermes

$F_2^p, \; F_2^d$

World data fits

$\sigma^{p,d}$ σ^d / σ^p

Gottfried Sum

$\int \frac{dx}{x}(F_2^p - F_2^n)$

d_v / u_v

Basic nucleon structure from sum rules

Quark-Parton Model

Adler sum rule

$$\int dx/x\,(F_2^{\bar{\nu}p}-F_2^{\nu p}) \;=\; \int dx/x\,(F_2^{\bar{\nu}n}-F_2^{\nu p}) \;=\; 2\int dx\,(u_v-d_v) \;=\; 2$$

← Sensitive to difference between u and d valence quarks

Gross-Llewellyn Smith sum rule

$$\int dx\,(F_3^{\bar{\nu}p}+F_3^{\nu p}) \;=\; \int dx\,(F_3^{\bar{\nu}n}+F_3^{\nu p}) \;=\; 2\int dx\,(u_v+d_v) \;=\; 6$$

← Sensitive to sum of u and d valence quarks

Gottfried sum rule

. . . .

Basic nucleon structure from sum rules

Quark-Parton Model

Adler sum rule

$$\int dx/x\,(F_2^{\bar{\nu}p}-F_2^{\nu p}) = \int dx/x\,(F_2^{\bar{\nu}n}-F_2^{\nu p}) = 2\int dx\,(u_v-d_v) = 2$$

← Sensitive to difference between u and d valence quarks

Gross-Llewellyn Smith sum rule

$$\int dx\,(F_3^{\bar{\nu}p}+F_3^{\nu p}) = \int dx\,(F_3^{\bar{\nu}n}+F_3^{\nu p}) = 2\int dx\,(u_v+d_v) = 6$$

← Sensitive to sum of u and d valence quarks

Gottfried sum rule

$\bar{u}=\bar{d}$

$$\int dx/x\,(F_2^{e,\mu p}-F_2^{e,\mu n}) = \frac{1}{3}\int dx\,(u_v-d_v) + \frac{2}{3}\int dx\,(\bar{u}-\bar{d}) \stackrel{\downarrow}{=} \frac{1}{3}$$

- Gottfried sum rule (charged lepton scattering) $\rightarrow$ Sensitive to
  - Difference between u and d valence quarks
  - **Sea quark flavor symmetry / asymmetry?**

Sea quark asymmetry

Measurements, e.g:

DIS data : SLAC, BCDMS, NMC, HERMES
Drell-Yan data: E288, (E772), NA51, E866

E.g.: NMC(Q^2=4 GeV^2): $I_G(0.004,0.8) = 0.236\pm0.008$
Extrapolation: $I_G(0,1) = 0.258\pm0.017$
→ Significant **violation of Gottfried sum rule**
Sea flavor asymmetry $\bar{u} \neq \bar{d}$. $I_G(0,1) < 1/3$: excess of $\bar{d}$ quarks over $\bar{u}$ quarks.

$\bar{d}$ quark excess confirmed in Drell-Yan and semi-inclusive analysis:

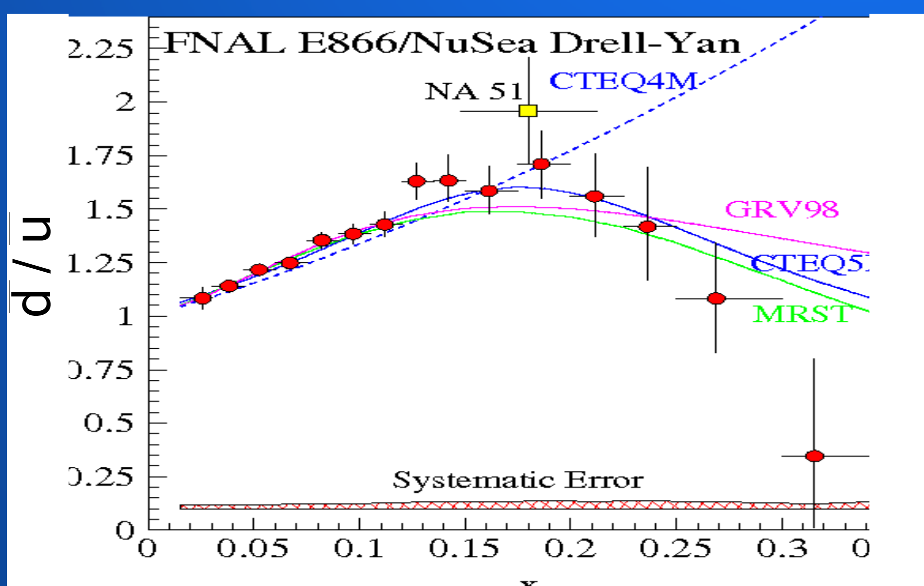

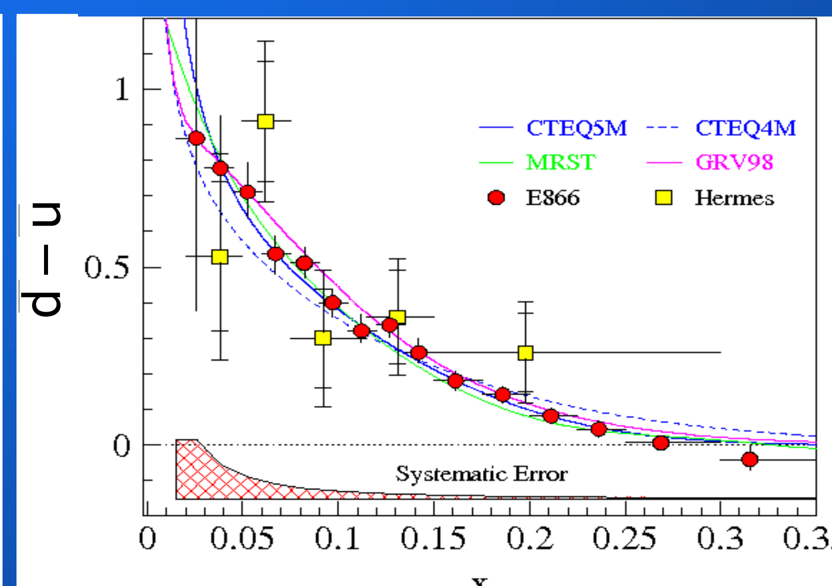

The Gottfried Integral

$$I_G(x_{min}, x_{max}) = \int_{xmin}^{xmax} (F_2^p(x) - F_2^n(x))\, dx/x \;=\; \int_{xmin}^{xmax} 2(F_2^p - F_2^d)\, dx/x$$

$$= \int_{xmin}^{xmax} 2\, F_2^p \left(1 - \frac{F_2^d}{F_2^p}\right) dx/x$$

Fit to F_2^p

Fit to σ^d/σ^p

Evaluation of the **measured** Gottfried Integral:

GD 08

Fit to σ^d/σ^p

Evaluation of the **leading twist (LT)** Gottfried integral

CTEQ6L

Fit to σ^d/σ^p (LT)

Fits to σ^d/σ^p

$$\frac{\sigma^d}{\sigma^p} \simeq \frac{F_2^d}{F_2^p}\left(1-\frac{1-\epsilon}{(1+\bar{R}(x))(1+\epsilon\bar{R}(x))}\Delta R(x)\right)$$

Relation of cross-section ratio to F_2-ratio

$$\frac{F_2^d}{F_2^p} \simeq \frac{F_2^{d,\mathrm{LT}}}{F_2^{p,\mathrm{LT}}}(x,Q^2)\left(1+\frac{C^d(x)-C^p(x)}{Q^2}\right)$$

Higher twist effects

$$\frac{F_2^{d,\mathrm{LT}}}{F_2^{p,\mathrm{LT}}}(x,Q^2) \simeq b_1(x)+b_2(x)\ln Q^2$$

Q^2 evolution

Parameterization

$$\frac{\sigma^d}{\sigma^p} \simeq \frac{F_2^d}{F_2^p}\left(b_1(x)+b_2(x)\ln Q^2\right)\left(1+\frac{C^d(x)-C^p(x)}{Q^2}\right)\left(1-\frac{1-\epsilon}{(1+\bar{R}(x))(1+\epsilon\bar{R}(x))}\Delta R(x)\right)$$

- **4-parameter Fit** in each *x* bin
  based on world data from **NMC, SLAC, BCDMS, HERMES**

World data on σ^d/σ^p

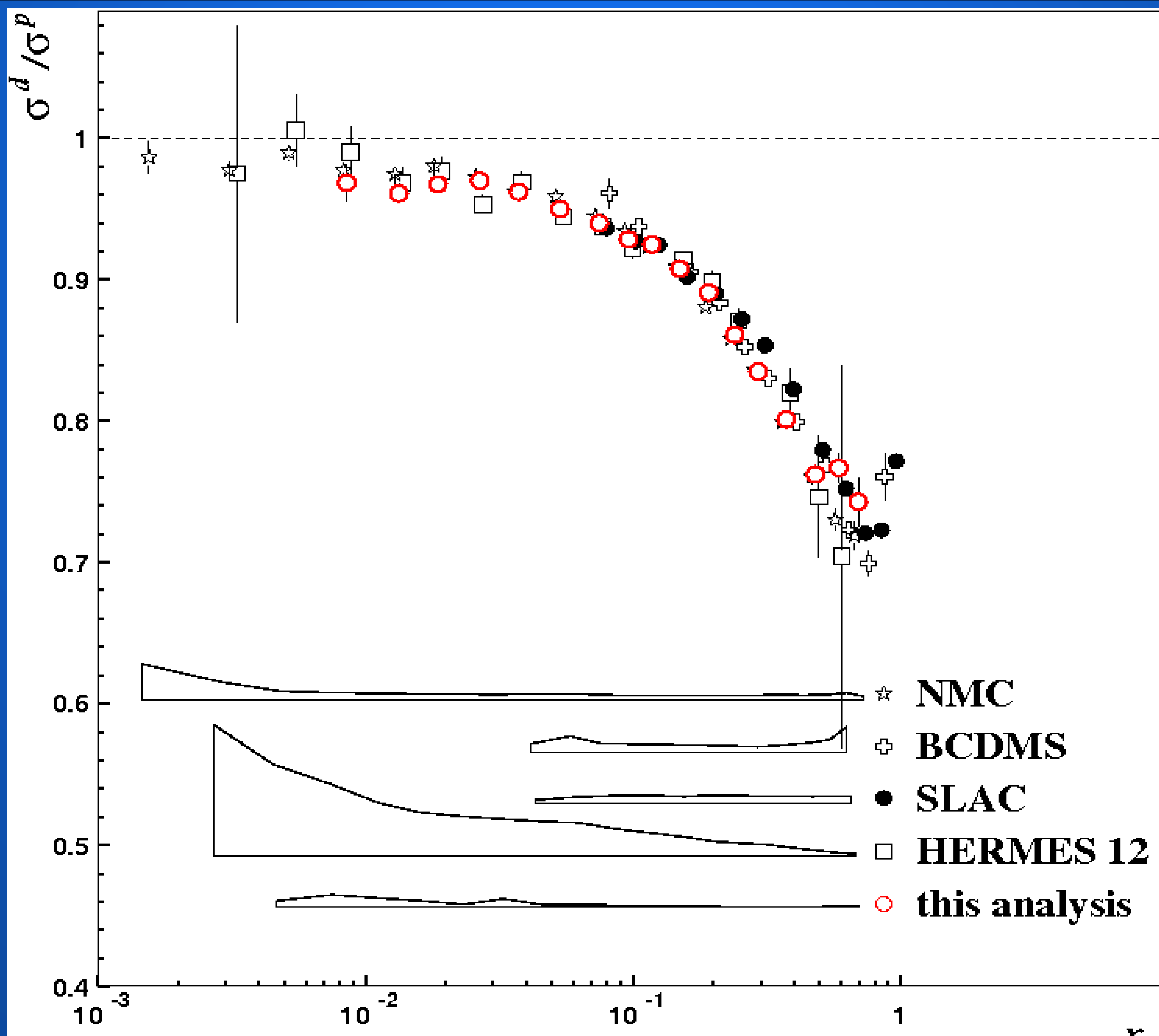

4 Parameters from Fit of σ^d/σ^p to world data

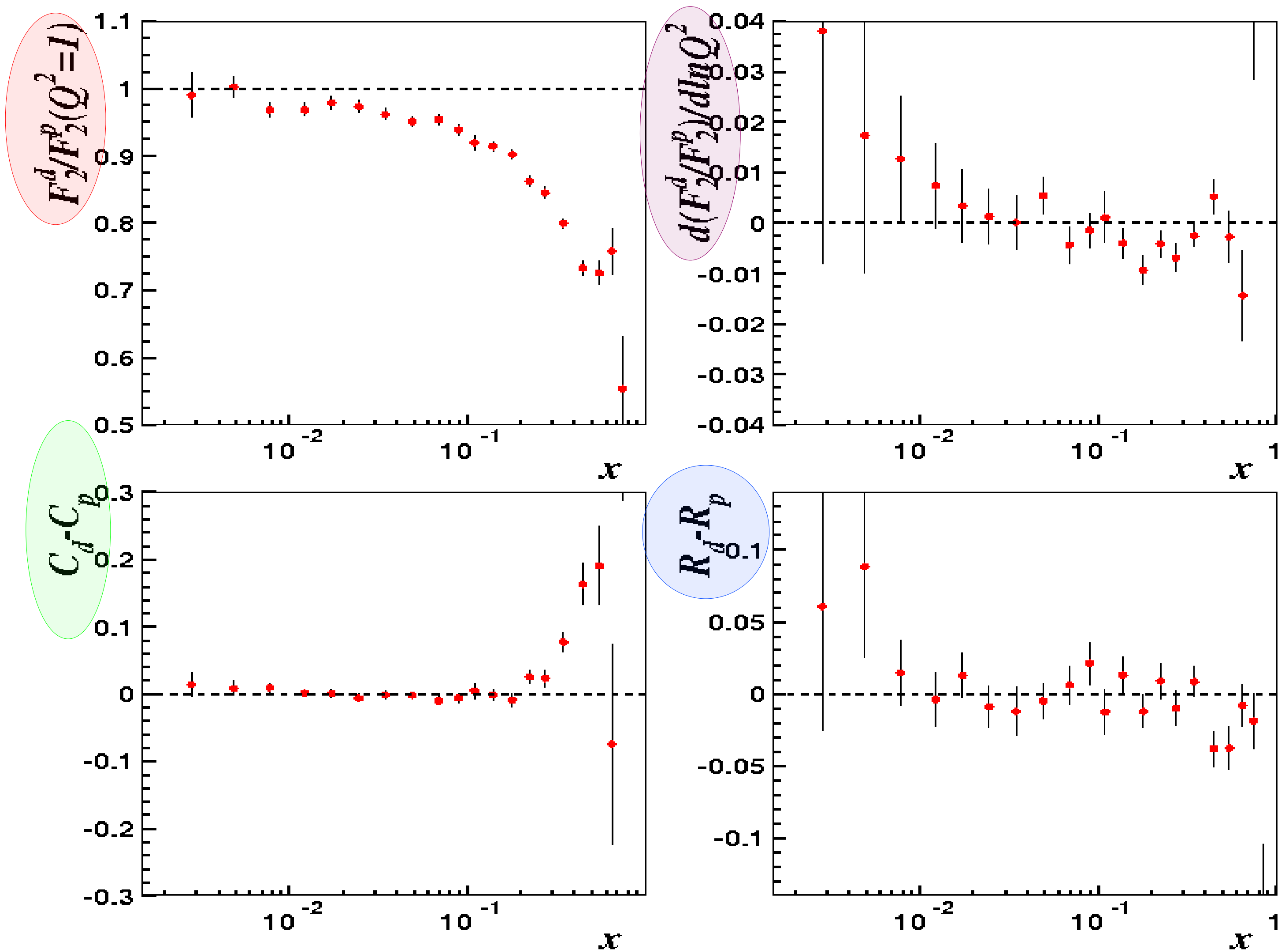

- $F_2^d/F_2^p(Q^2=1)$: approaching unity for small x.
- $d(F_2^d/F_2^p)/dlnQ^2$: tendency to negative slopes at high x.
- $C_d - C_p$: significant only at x>0.2
- $R_d - R_p$: Consistent with zero

Evaluation of the Gottfried integral

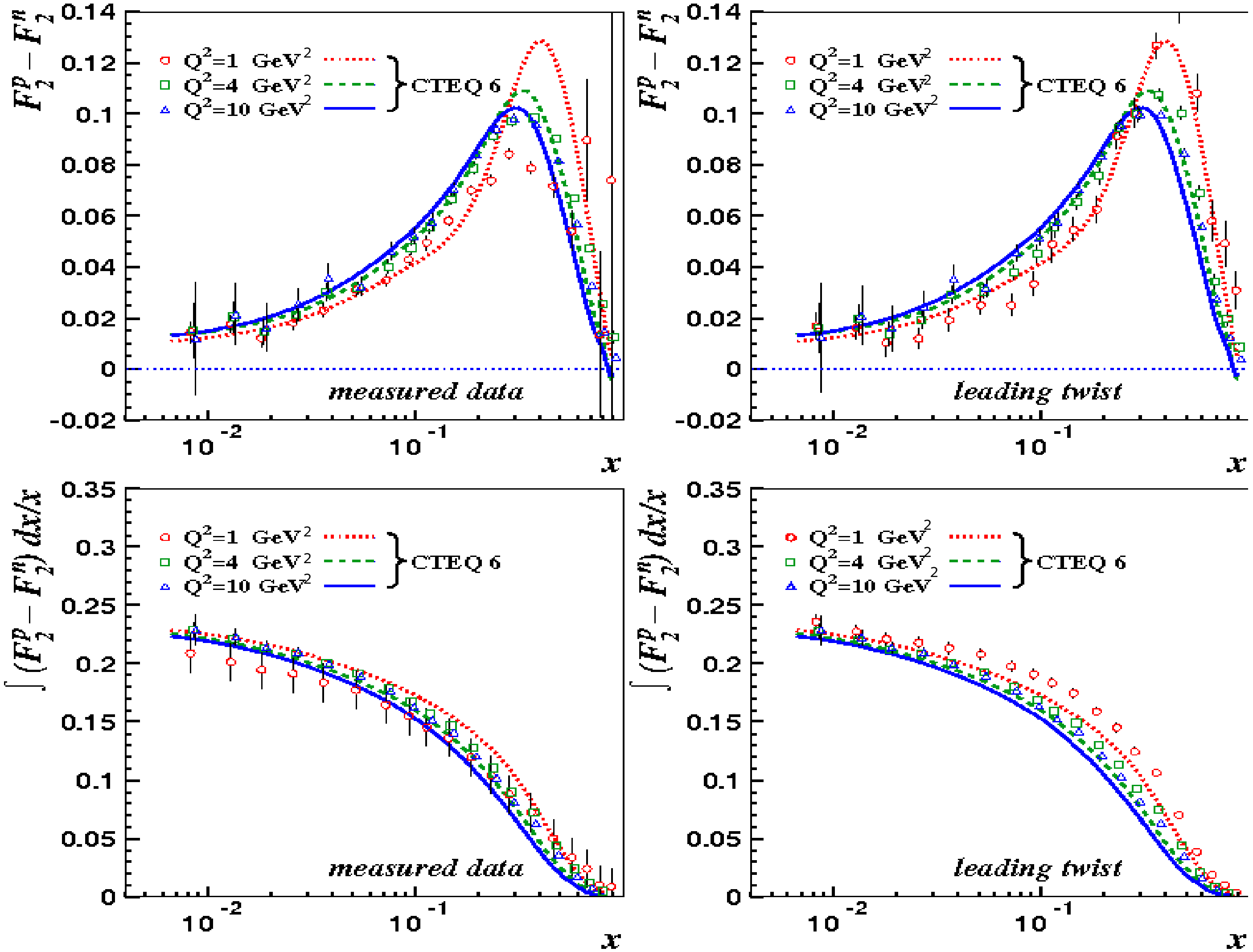

Q^2	x - range	$I_G^{meas.}$	I_G^{LT}
1 GeV²	0.006-0.9	0.208±0.016	0.236±0.006
4 GeV²	0.006-0.9	0.228±0.006	0.228±0.006
10 GeV²	0.006-0.9	0.228±0.013	0.228±0.012

Extraction of d_v/u_v

Extraction of d_v/u_v

$$\frac{F_2^d}{F_2^p} = \frac{1}{2}\left(1 + \frac{F_2^n}{F_2^p}\right) \simeq \frac{1}{2}\left(1 + \frac{4\frac{d_v}{u_v} + 1 + S_1}{4 + \frac{d_v}{u_v} + S_2}\right) \overset{S_{1,2}=0}{\approx} \frac{5}{2} \cdot \frac{1 + \frac{d_v}{u_v}}{4 + \frac{d_v}{u_v}}$$

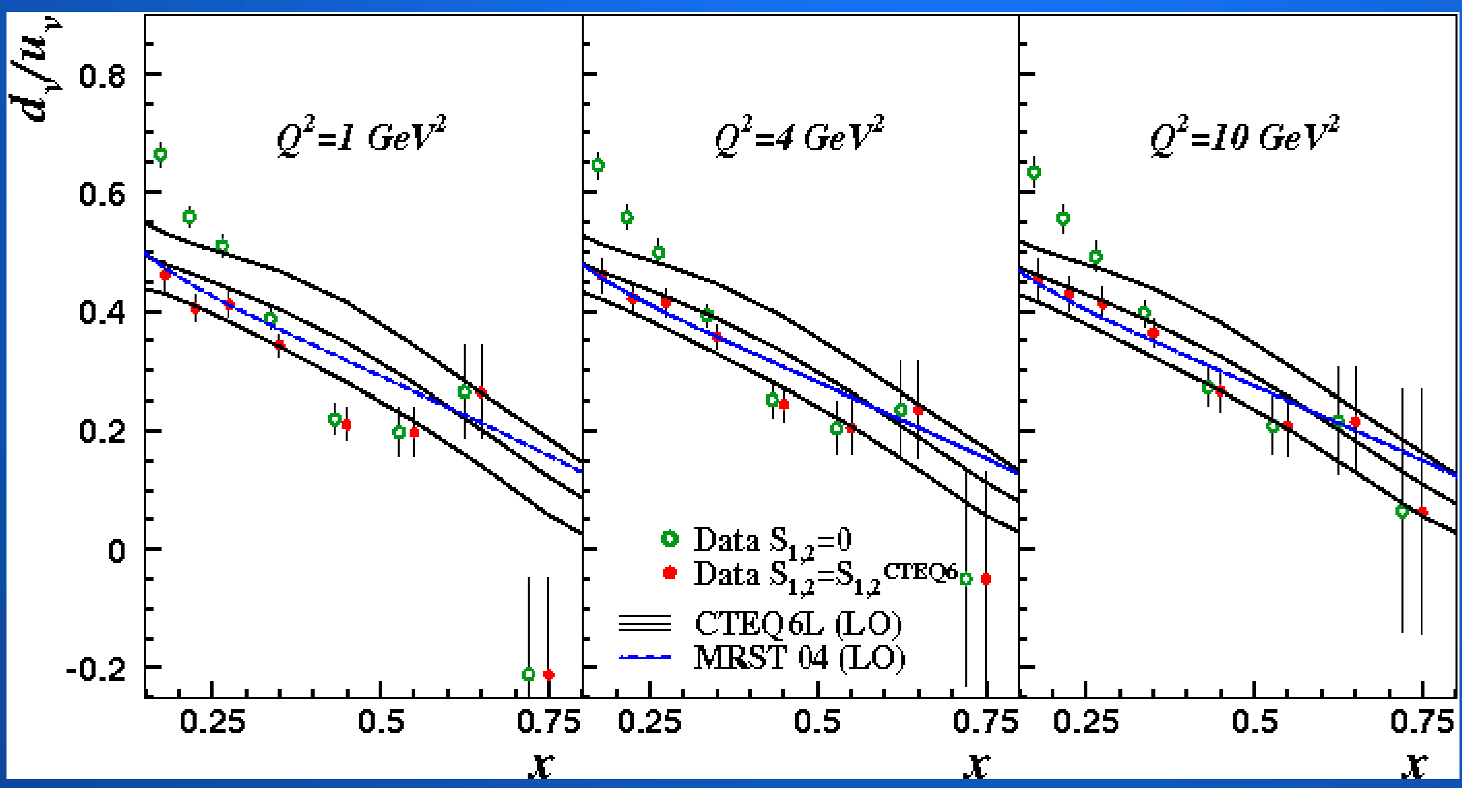

$$S_1 = \frac{2}{u_v}(u_s + 4d_s + s_s)$$

$$S_2 = \frac{2}{u_v}(4u_s + d_s + s_s)$$

- S_1 and S_2 taken from CTEQ6L
- Impact of S_1 and S_2 negligible at x>0.35

- Comparison of dv/uv with CTEQ6L (LO) result reveals compatibility.

Summary

- First measurement of F_2^p and F_2^d at Hermes.

- Fit of the proton DIS cross section based on the ALLM functional form
  - Larger data set, 2821 data points, incl. Hermes
  - Self-consistent with respect to R
  - Normalization uncertainties taken into account
  - Covariance matrix provided

- Fit of the cross section ratio σ^d/σ^p
  - Extraction of the Gottfried integral
  - Compatibility with the NMC result
  - Indicates violation of Gottfried sum rule
  - No indication for Q^2 dependence found